Investigating Induced Pluripotent Stem Cells for Tissue Engineering and Hepatotoxicity Applications

Lauren R. Wills

Thesis submitted to the faculty of the Virginia Polytechnic Institute and State University in partial fulfillment of the requirements for the degree of

Master of Science in
Biomedical Engineering

Padmavathy Rajagopalan, Chair
Yong Woo Lee
Pamela VandeVord

May 6, 2019
Blacksburg, VA

Keywords: induced pluripotent stem cell, hepatocytes, toxicity, organotypic *in vitro* models

Investigating Induced Pluripotent Stem Cells for Hepatotoxicity Applications

Lauren R. Wills

ABSTRACT

Induced pluripotent stem cells (iPSCs) can be differentiated into multiple cell types in the body while maintaining proliferative capabilities. The generation of human iPSC-derived hepatocytes (iPSC-Heps) has resulted in a new source for hepatic cells. The current available options for human hepatocytes are primary human hepatocytes (PHHs) and cell lines. PHHs isolated from healthy human donors are difficult to obtain, while cell lines exhibit reduced hepatotoxic sensitivity. iPSC-Heps are being investigated as an alternative option as they are derived from a continuous, stable source and are able to maintain their original donor genotype, which opens the door for patient-specific studies. iPSC-Heps show promise for utilization in tissue engineering, hepatotoxicity studies as well as screening for patient-specific therapeutics. Various reports have concluded that iPSC-Heps exhibit reduced hepatocyte function in comparison to PHHs. Prior reports on iPSC-Heps have focused on improving their adult phenotype functions through variations in differentiation protocols or by altering their *in vitro* culturing environment. This thesis focuses on incorporating hepatic non-parenchymal cells to more closely mimic the tissue and cell architecture found in the liver tissue. We designed and assembled a 3D iPSC-Hep model that integrates liver sinusoidal endothelial cells, with the goal of achieving functional maturity. Hepatotoxicants were administered to our models and various hepatic markers were measured to analyze the toxic response. This work demonstrates the need for the inclusion of hepatic non-parenchymal cells in iPSC-derived liver tissues, specifically for hepatotoxicity applications.

Investigating Induced Pluripotent Stem Cells for Hepatotoxicity Applications

Lauren R. Wills

GENERAL AUDIENCE ABSTRACT

Induced pluripotent stem cells (iPSCs) can be differentiated into multiple cell types in the body while maintaining proliferative capabilities. The generation of human iPSC-derived hepatocytes (iPSC-Heps) has resulted in a new source for hepatic cells. The current available options for human hepatocytes are primary human hepatocytes (PHHs) and cell lines. PHHs originating from healthy human donors are difficult to obtain, while cell lines may exhibit reduced hepatotoxic sensitivity to chemicals. iPSC-Heps are being investigated as an alternative option since they are derived from a continuous source and are able to maintain their original donor genetic make-up, allowing for patient-specific studies. iPSC-Heps can be used in tissue engineering, hepatotoxicity studies as well as screening for patient-specific therapeutics. Various reports have concluded that iPSC-Heps exhibit reduced function in comparison to PHHs. Prior reports on iPSC-Heps have focused on improving their function through variations in differentiation procedures or by changing their culture environment. This thesis focuses on incorporating other hepatic cells to more closely mimic the tissue and cell architecture found in the liver tissue. We designed and assembled a 3D iPSC-Hep model that integrates liver sinusoidal endothelial cells, with the goal of improving hepatocyte function. Chemicals were administered to our models and various hepatic markers were measured to analyze the toxic response. This work demonstrates the need for the inclusion of additional hepatic cell types in iPSC-derived liver tissues, specifically for hepatotoxicity applications.

Acknowledgements

I would like to thank my advisor, Dr. Padma Rajagopalan, for everything she has taught me over the past 3 years. She constantly challenged me to work harder and deepen my scientific understanding, and as a result I have truly grown as a researcher. I appreciate her willingness and patience to answer my never-ending list of questions and for always encouraging me to ask more. She has put in countless hours not only discussing my project and helping me with my experiments, but also being there as a life mentor to guide me and help me grow as a person. I would also like to thank my committee members Dr. Pamela VandeVord and Dr. Yong Woo Lee for their valuable input and feedback on my thesis.

I would like to thank my fellow lab members Diego Almodiel, Neeladri Chowdhury, Dr. Andrew Ford, Rosalyn Hatlen, Anjaney Kothari, and Dr. Sophia Orbach for all of their assistance and for making the lab an enjoyable place. I would especially like to thank Dr. Sophia Orbach for training me and being an excellent teacher who I could always rely on for support.

To my family, for all of your love and encouragement, I would not have succeeded without you and I am forever grateful for your support. To my friends Andrea, Gabby, Rachael, and Ryan, thank you for always being there, your friendship has meant the world to me.

Lastly, I would like to acknowledge financial support from the National Science Foundation, the ICTAS VCOM Research Eureka Acceleration Program, the Institute for Critical Technologies and Applied Sciences at Virginia Tech, and the Computational Tissue Engineering Graduate Education Program at Virginia Tech.

Table of Contents

List of Figures

List of Abbreviations

3DHL – 3D hepatocyte-LSEC culture
AAT - alpha-1-antitrypsin
AFP - alpha-fetoprotein
AHS - Alpers-Huttenlocher syndrome
APAP - acetaminophen
ASGPR - asialoglycoprotein receptor
BMP - bone morphogenic protein
BSA – bovine serum albumin
CS – collagen sandwich
CYP - cytochrome P450
DILI - drug-induced liver injury
ECGS – endothelial cell growth supplement
ECM - extracellular matrix
EDTA - ethylenediaminetetraacetic acid
ESC - embryonic stem cell
EtOH - ethanol
FBS – fetal bovine serum
FGF - fibroblast growth factor
GSH – glutathione
HFC - 7-hydroxy-4-trifluoromethylcoumarin
HGF - hepatocyte growth factor
HNF4α - hepatocyte nuclear factor 4-alpha
HSC - hepatic stellate cell
iPSC - induced pluripotent stem cell
iPSC-Hep - induced pluripotent stem cell derived hepatocyte
ICM - inner cell mass
LDH – lactate dehydrogenase
LDL - low-density lipoprotein
LDL-C - low-density lipoprotein cholesterol
LDLR - low-density lipoprotein receptor
LSEC - liver sinusoidal endothelial cell
M-CSF - macrophage colony stimulating factor
MFC - 7-methoxy-4-trifluoromethylcoumarin
MPCC – micro-patterned co-culture
mPTP - mitochondrial permeability transition pore
NAPQI - *N*-acetyl-*p*-benzoquinone imine
NPC - non-parenchymal cell
PBS – phosphate buffered saline
PHH - primary human hepatocyte
PLLA – poly-L-lactic acid
PSC - pluripotent stem cell
RIN – RNA integrity number
ROS - reactive oxygen species
SDS – sodium dodecyl sulfate
SNP - single nucleotide polymorphism
TCPS – Tissue culture polystyrene
VEGF - vascular endothelial growth factor
VPA - valproic acid

Chapter 1: Literature Review

1.1 Introduction

1.1.1 Induced Pluripotent Stem Cells (iPSCs)

A pluripotent stem cell (PSC) is a cell that has the ability to differentiate into any cell type derived from one of the three germ layers: endoderm, mesoderm, and ectoderm [1-3]. PSCs originate within embryos, and are specifically referred to as embryonic stem cells (ESCs) [2, 4]. ESCs are formed during embryogenesis in the blastocyst stage [5, 6]. The blastocyst is comprised of trophoblast cells that make up the outer shell and an inner cell mass (ICM) containing cells with pluripotent capabilities [4, 7]. The ICM can yield all cells found in the adult human body [3, 4, 6]. During embryonic development, cells first exhibit totipotent abilities in the zygote and become increasingly differentiated until they reach a final somatic cell phenotype [7, 8]. Although, it is possible to revert somatic cells back to pluripotency by either nuclear transfer, cell fusion, or direct reprogramming [8, 9]. Induced pluripotent stem cells (iPSCs) are obtained by the method of reprogramming terminally differentiated cells back to a pluripotent state [2, 9].

iPSCs were first generated by Takahashi and Yamanaka in mouse fibroblasts in 2006, followed by human iPSCs in 2007 [10, 11]. Mouse iPSCs were produced by introducing a set of four genes, Oct4, Sox2, Klf4, and c-Myc, through retroviral transduction [11]. Utilizing the exact same set of four transcription factors, human iPSCs were generated from dermal fibroblasts [10]. To arrive at this particular set of transcription factors, an initial set of 24 genes that were involved in the maintenance of ESCs were analyzed [11]. It was concluded that this specific set of four genes produced the best results [11]. Oct4 and Sox2 were identified as necessary for the successful generation of iPSCs [11]. Oct4 helps the development of the ICM, and its' absence can cause cells to lose their pluripotency and differentiate into trophoblast cells [5, 9]. In addition to maintaining pluripotency, Sox2 is linked to ESC self-renewal [9]. The first human iPSCs mimicked

ESCs in many aspects, including the expression of surface antigens, gene expression, proliferation time, morphology, teratoma formation and telomerase activity, while also demonstrating the ability to differentiate into cells derived from all three germ layers [10]. Since the first successful attempt completed by Takahashi and Yamanaka, several other groups have succeeded in generating both mouse and human iPSCs and improving the process of reprogramming [12-19]. Studies were conducted to generate iPSCs without the use of c-Myc, since it increases the potential for tumor formation [17]. Nakagawa *et al.* reported the formation of iPSCs when c-Myc was omitted, but the total yield was found to be ~13 times lower [14]. It was also stated iPSCs could only be obtained in about half of the experiments when not utilizing c-Myc [14]. Yu *et al.* reported that a combination of Oct4, Sox2, Nanog, and Lin-28 also lead to the production of iPSCs [13]. Questions have been raised as to the similarity of iPSCs to ESCs. Various reports stated that iPSCs do have genetic differences from ESCs, while other studies indicated these discrepancies may be due to experimental inconsistencies [20]. No major functionality differences between iPSCs and ESCs have been reported, so the gene expression differences have not yet resulted in any noticeable physiologic impact [21].

Many of the early protocols for generating iPSCs utilized viral vectors, which permanently alters the genetic makeup of the cell by integrating into the genome (**Figure 1.1**) [22]. Uses of the non-integrating adenovirus [23] and recombinant proteins [24, 25] demonstrated that genome manipulation was not necessary. Although, none of these approaches were able to improve upon the efficiency of generating iPSCs [20, 22]. Alternatively, small molecules have been incorporated into reprogramming protocols to be used in conjunction with transcription factors (**Figure 1.1**) [12, 26, 27]. This method proved useful at replacing the need for either one or two of the original four transcription factors [28]. Shi *et al.* succeeded in producing iPSCs through use of Oct4 and Klf4 supplemented with BIX-01294 [12], while Huangfu *et al.* combined Oct4, Sox2, Klf4, and valproic acid (VPA) [26]. An advantage of the small molecule method is improved production efficiency

[28]. Huangfu *et al.* reported a 50-fold increase in reprogramming efficiency with VPA treatment [26].

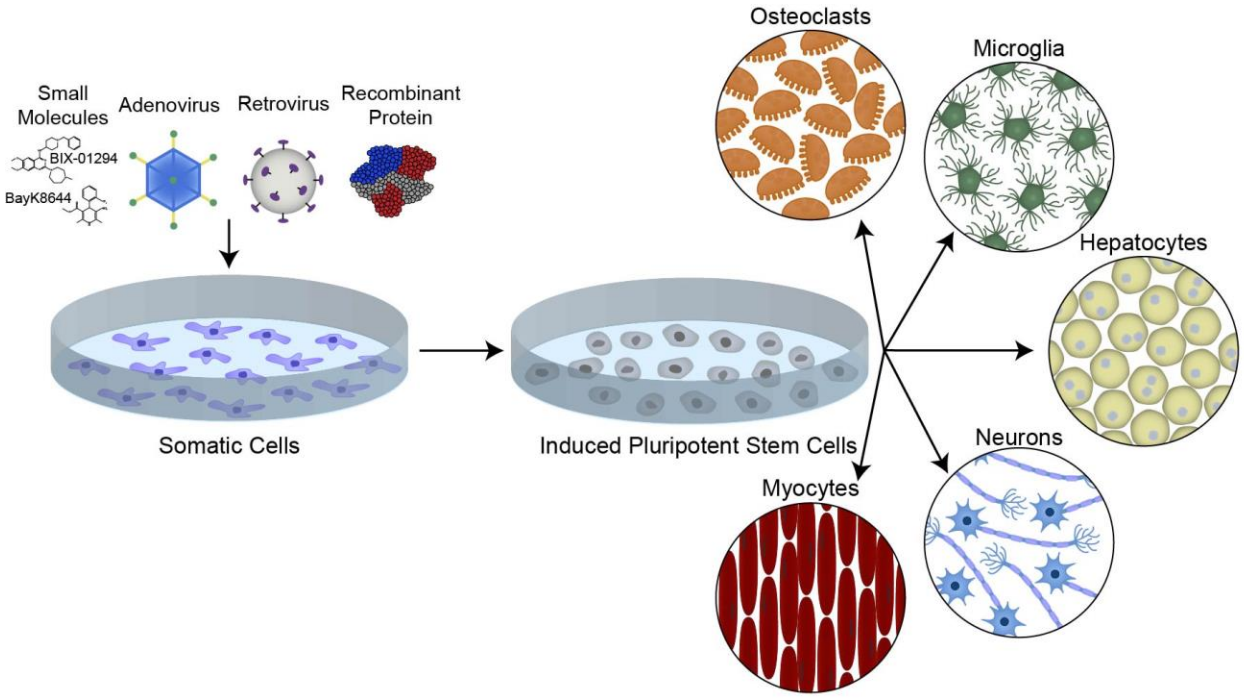

Figure 1.1: Schematic showing the reprogramming of somatic cells to iPSCs and further differentiation to other cell types. Somatic cells can be reprogrammed through utilization of retroviruses, adenoviruses, recombinant proteins, or small molecules to obtain an iPSC phenotype. iPSCs can then be differentiated to different cell types.

iPSCs are critical to enhance our current understanding on how stem cells function and behave. Although there are several reports in the literature on the use of ESCs, ethical and sourcing issues have resulted in obstacles for the scientific community. Human iPSCs have been used to obtain skeletal muscle tissue [29], microglia cells [30], cardiomyocytes [31-33], neural cells [34-36], and osteogenic cells [37-39] (**Figure 1.1**). The scope and potential for iPSCs are tremendous. In this review, we focus our attention on hepatic cells obtained from iPSCs, the need for such cells, as well as their applications in hepatotoxicity studies.

1.2 Hepatic Cells Derived From iPSCs

1.2.1 Cellular Composition of the Liver

The liver plays an integral role in metabolism, protein synthesis and in numerous physiological functions [40, 41]. The principal cells are hepatocytes that comprise about 80% of the liver mass and perform several metabolic function [40]. In addition to hepatocytes the other primary cell types are liver sinusoidal endothelial cells (LSECs), Kupffer cells, and hepatic stellate cells (HSCs) [40, 41]. LSECs line the sinusoid and exhibit fenestrae [40]. Kupffer cells are the resident macrophages of the liver [40, 42]. HSCs reside in the space of Disse and store vitamin A when quiescent [40, 42].

1.2.2 Hepatocyte like cells obtained from iPSCs (iPSC-Heps)

Many protocols have been developed to differentiate iPSCs to hepatocyte like cells (defined henceforth as iPSC-Heps) [43]. These procedures involve a chronological addition of supplements to promote step-wise differentiation towards hepatocytes [43]. The definitive endoderm is targeted first, followed by hepatic differentiation, and then hepatocyte maturation [43]. Researchers have frequently supplemented culture medium with Activin A and Wnt3A (endoderm), fibroblast growth factor (FGF), bone morphogenetic protein (BMP) (hepatic specific), hepatocyte growth factor (HGF), oncostatin M and dexamethasone (hepatic maturation) (**Figure 1.2**) [43]. One differentiation strategy is to aggregate iPSCs into embryoid bodies, forming 3D structures that help mimic the cell-cell interactions that occur during development [44]. However, the embryoid body technique can also result in the spontaneous differentiation to additional cell types [44]. Other procedures to improve the differentiation process involve the removal of serum, feeder cells and other undefined media components [45]. Si-Tayeb *et al.* found that their method of only using defined culture conditions led to a highly efficient differentiation method that resulted in 80-85% of cells expressing albumin [45]. iPSC-Heps have been shown to exhibit hepatic markers such as glycogen storage, albumin secretion, urea synthesis, hepatocyte morphology, and cytochrome P450 (CYP) expression [45-49]. Although, these cells are hepatocyte-like, there

are significant differences in their enzyme expression and cellular function when compared to PHHs [45, 46, 50].

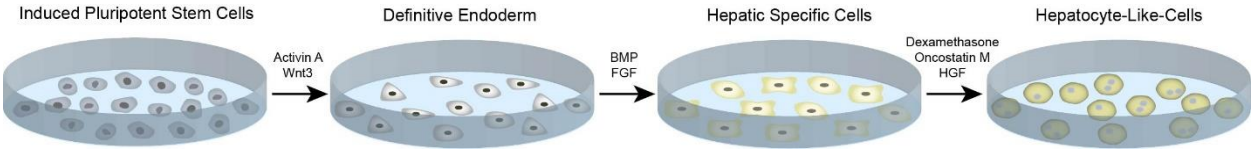

Figure 1.2: Schematic depicting procedures to differentiate iPSCs to hepatocytes. Many groups have developed protocols to differentiate hepatocytes from iPSCs. To differentiate iPSCs to definitive endoderm Activin A and Wnt3 are commonly administered. Bone morphogenic protein (BMP) and fibroblast growth factor (FGF) are added to the endodermal cells to induce hepatic differentiation. To achieve hepatocyte maturation, dexamethasone, oncostatin M, and hepatocyte growth factor (HGF) are frequently used as supplements.

Recognizing the differences between iPSC-Heps and adult hepatocytes, efforts have been made in culture conditions and to improve the stage-wise differentiation protocols to obtain more mature hepatocytes. One approach focused on hepatocyte necrosis factor 4 alpha (HNF4α) transduction with an adenovirus vector during the hepatoblast stage [51]. iPSC-Heps transduced with HNF4α exhibited increased gene expression of six CYPs as opposed to cells differentiated without the HNF4α factor [51]. Studies have been conducted wherein iPSCs formed 3D aggregates after partial hepatocyte differentiation had begun, to promote their maturation and polarity [52, 53]. In combination with 3D cultures, specific pathways important to liver development have been targeted. For example, the inhibition of the Wnt/β-catenin pathway resulted in mature cells, however, the iPSC-Heps formed using this approach exhibited albumin secretion that was approximately 60% obtained from PHH cultures [54]. Another approach used to improve the functions of iPSC-Heps was to co-culture with either iPSC-derived LSECs and HSCs [55], or Swiss 3T3 murine fibroblasts [56].

Various efforts have also been made to improve the hepatic function of iPSC-Heps after they are differentiated, through employing unique *in vitro* models. A 2D micro-patterned co-culture (MPCC) model confined iPSC-Hep attachment to collagen coated islands surrounded by murine

fibroblasts (**Figure 1.3A**) [57]. iPSC-Heps cultured in MPCCs performed better than monolayers in terms of albumin and urea secretion, gene expression of nuclear receptors, and expression of CYPs. In addition, this study demonstrated that when iPSC-Heps were cultured in MPCCs, CYP2C9 and CYP3A4 enzymes responded to induction by rifampicin and phenobarbital. This improvement was attributed to homo and heterotypic cellular interactions. Another strategy was to seed iPSC-Heps directly onto a 3D scaffold [58]. Wang *et al.* prepared scaffolds composed of either decellularized rat liver ECM or a 3D printed poly-L-lactic acid construct that was coated with type 1 collagen (**Figure 1.3B**) [58]. They reported that cells seeded on the ECM scaffold had a significant increase in albumin production for the duration of the culture and AFP synthesis was significantly reduced after 7 days relative to a control sandwich culture. Wang *et al.* reported the ECM scaffold also significantly increased the activity of CYP2C9, 3A4, and 1A2, and showed that all 3 CYPs were capable of responding to induction [58]. When comparing the CYP activity to PHHs in the ECM scaffold at day 14, the iPSC-Heps in the ECM scaffold exhibited activity that was similar to that of PHHs for CYP1A2 and ~2.5-fold higher for CYP3A4 [58]. Another technique involved the formation of a multi-interfacial polyelectrolyte complex [59]. Du *et al.* differentiated both hepatocytes and endothelial cells from iPSCs. Each cell type was then added to a chitin solution that was combined with either galactose (hepatocytes) or collagen-I (endothelial cells). The resulting hydrogel fiber encapsulated the cells in their individual domains. Albumin secretion in the co-cultures was approximately 2-4 fold higher than values obtained from hepatocyte cultures.

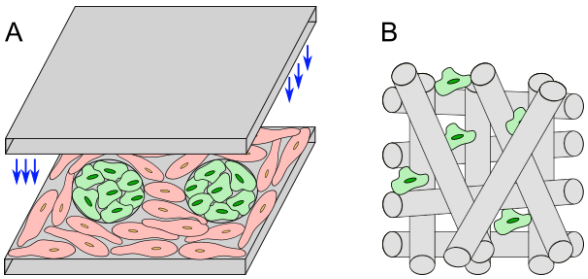

Figure 1.3: Schematic of in vitro cultures to improve iPSC-Hep functions, (**A**) MPCC cultures and (**B**) 3D poly-L-lactic acid-collagen coated scaffold.

In summary, iPSC-Heps have been shown to secrete albumin and urea, participate in the uptake low-density lipoprotein (LDL), maintain the typical hepatocyte polygonal morphology with binucleated cells, store glycogen, express liver markers such as asialoglycoprotein receptor (ASGPR), α-1-antitrypsin (AAT), and HNF4a, form tight junctions and form bile canaliculi [57, 60-62].

1.2.3 iPSC-derived Hepatic Non-Parenchymal Cells

The three primary non-parenchymal cells (NPCs) of the liver have also successfully been differentiated from iPSCs (**Figure 1.4**). To generate iPSC-derived LSECs, mesoderm differentiation was first targeted [55]. Thereafter, vascular endothelial growth factor (VEGF) was administered to target an endothelial lineage. From the resulting cell population, only cells expressing three specific LSEC markers (FLK1, CD31, and CD34) were selected to continue the maturation process [55]. The addition of A83-01 differentiated the cells to an LSEC phenotype. A similar process also proved successful at generating HSCs [55]. Directly after mesoderm differentiation, the cells expressing the cell surface marker ALCAM were selected to be further matured into HSCs. The maturation step involved the addition of Y27632 to obtain an HSC phenotype. An alternative protocol for HSC differentiation utilized BMP and FGF (**Figure 1.4**) [63]. To obtain a mature HSC phenotype the cells were cultured with retinol and palmitic acid. The protocol to yield Kupffer cells first targeted macrophage precursor differentiation with interleukin-3 and macrophage colony stimulating factor (M-CSF) [64]. M-CSF was also used in the following step to yield primitive macrophages. The final differentiation step involved the use of primary human hepatocyte conditioned media to obtain Kupffer cells.

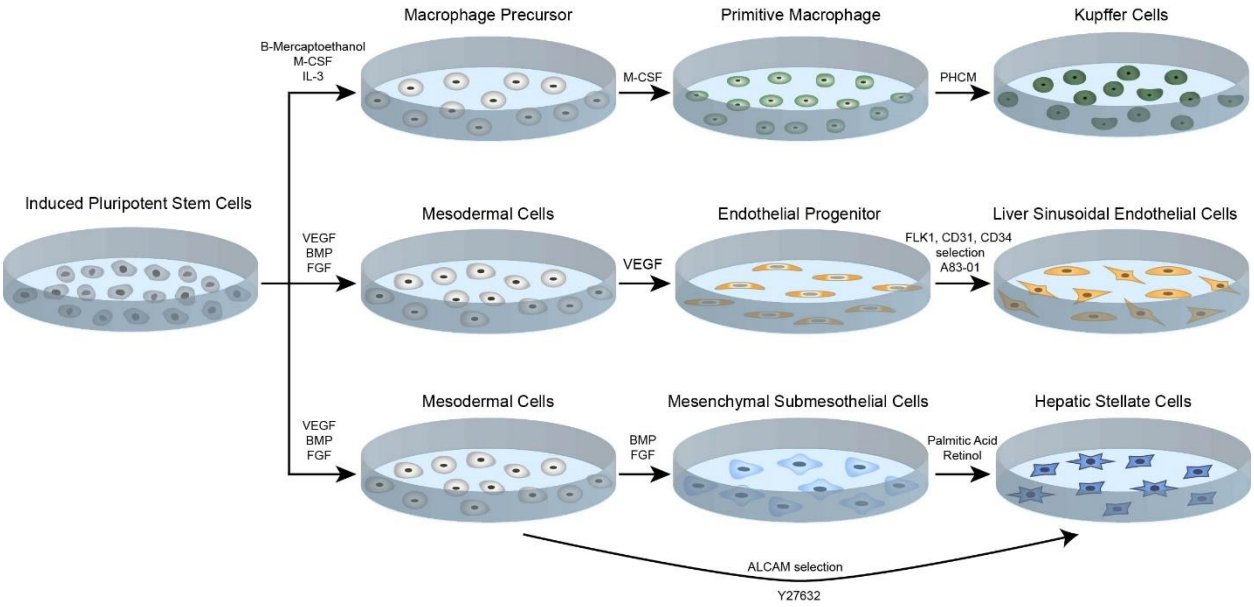

Figure 1.4: Schematic depicting procedures to obtain non-parenchymal hepatic cells from iPSCs.

1.3 Hepatotoxicity Evaluations

Biotransformation is one of the vital functions of the liver [40, 41]. Cytochrome P450 enzymes (CYPs) are Phase I enzymes that are responsible for the biotransformation for several drugs, xenobiotics and chemicals. CYP1A2, CYP2C9, CYP2C19, CYP2D6, and CYP3A4, are primarily responsible for many drugs metabolized by CYPs [65]. The exposure of the liver to harmful chemicals can result in drug-induced liver injury (DILI), which is the leading cause of acute liver failure [65]. Not all people respond to drugs in the same manner due to polymorphisms in the CYP genes leading to idiosyncratic DILI[65] . In later sections, we describe how iPSC-Heps may be used to provide information on patient-specific liver toxicity.

For *in vitro* toxicity evaluations using human cells, both cell lines and primary cells have been utilized. Among cell lines, Huh7, Fa2N-4, HepG2, Hep3B, and HepaRG are frequently studied; with HepG2 being the most commonly utilized [42, 66, 67]. Cell lines are beneficial because they are inexpensive, proliferate when cultured and in general are easier to work with in comparison

to primary cells [68, 69]. However cell lines have often been genetically manipulated to obtain this proliferating ability and therefore differ from primary hepatic cells [68]. Generally, cell lines are known to have reduced enzyme expression levels, particularly for phase I and II drug metabolizing enzymes, and can dedifferentiate in culture at higher passage numbers [42, 66, 67, 69]. HepaRG, HepG2, and Huh7 cells are derived from hepatocarcinomas, leading to an altered metabolism [66, 70].

Since PHHs are obtained from human liver tissue there are wide-ranging benefits to using these cells. PHHs can exhibit metabolism and enzymatic activity that are closer to what is observed *in vivo* [42, 69], [67, 71, 72]. When cultured in a 3D spheroid, CYP activity and metabolomics stability was maintained up to 21 days [73]. Other reports in the literature have shown that 3D cultures, spheroids, microfluidic devices, and microscale bioreactors can significantly improve the functions of PHHs [74-76]. Despite the obvious benefits of working with PHHs, a significant concern is the reliance upon human donors to obtain these cells. Since PHHs are typically obtained from cadaverous tissues, they are limited in supply. In addition, there is a lot of variation based upon gender, age, lifestyle, and ethnicity [42, 77]. Such variations in donors can affect the outcomes of experimental studies conducted with PHHs [70].

1.3.1 iPSC-Heps in Hepatotoxicity Testing

iPSC-Heps are an emerging alternative to PHHs. Over the last few years several research groups have studied their liver functions as well as their ability to biotransform xenobiotics and toxicants [57, 58, 60-62, 78, 79]. It has been shown that iPSC-Heps express various CYP enzymes, phase II enzymes, and their functions have been compared to PHHs or human hepatic cell lines [61, 78, 80]. Ulvestad *et al.* analyzed CYP activity and drug transporter function over a week in culture for iPSC-Heps and compared them to PHHs [81]. iPSC-Heps exhibited almost no CYP2B6 (~ 0.2%) and CYP2C9 (~ 0.2%) activity relative to the PHHs at 4 hours in culture. iPSC-Heps primarily

expressed CYP3A5 and low levels of CYP3A4. The authors noted that in the future obtaining hepatocytes from stem cells with a defect 3A5 allele would be of interest.

An extensive transcriptomic study was conducted that compared iPSC-Heps to PHHs from six donors, HepaRG, Huh7, HepG2, and HepG2/CA3 cells [80]. In this study iPSC-Heps overexpressed CYP3A7, which is the fetal form of CYP3A whereas HepaRG and PHHs expressed the adult phenotypes, CYP3A4 and CYP3A5 [80]. Lu *et al.* reported that the basal expression of CYP1A2, CYP2B6 and CYP3A4 were lower than those detected in PHHs [60]. Medine *et al.* completed a drug sensitivity test that measured cell viability for two separate compounds, Bristol-Myers Squibb (BMS) 1 and 2, with PHHs, iPSC-Heps and ESC-derived hepatocytes [61]. BMS 1 administration caused no significant effect on viability and this was attributed to an absence of CYP2C9 activity in iPSC-Heps. CYP3A and CYP1A2 activities for iPSC-Heps were found to be approximately 34% and 1% of that observed in PHH cultures, respectively. Sjogren *et al.* reported iPSC-Heps did express various drug transporters, transcription factors, and phase II enzymes on levels similar to PHH expression such as PXR, CAR, and MRP2 [78]. Other genes were expressed at reduced levels relative to PHHs such as OAT4 and UGT2B7, while the iPSC-Heps had a higher expression of alpha-fetoprotein (AFP) [78]. In a comparison between PHHs, iPSC-Heps, HepaRG, and Huh7, iPSC-Heps exhibited similar sensitivity to staurosporine as PHHs. When acetaminophen was administered, *N*-acetyl-*p*-benzoquinone imine (NAPQI) formation was not observed in iPSC-Heps, which was attributed to the low expression of both CYP2E1 (0.2 %) and CYP3A4 (0.7 %) relative to PHHs.

Kang *et al.* observed that iPSC-Heps and PHHs exhibited sensitivity to APAP and aflatoxin B [62]. iPSC-Heps have also been used to study the toxicity of phytochemicals [82, 83]. PHHs, HepG2 cells, and iPSC-Heps were used to study the effects of different phytochemicals to study herbal hepatotoxicity [82]. A toxicity study was conducted with iPSC-Heps in MPCC cultures model that

included 47 liver toxins (e.g. APAP, Diclofenac, Isoniazid, Tamoxifen) and non-liver toxins (e.g. Aspirin, Prednisone, and Warfarin) [79]. When the same liver toxicants were administered to iPSC-Heps cultured in MPCC cultures, the sensitivity to liver toxins was found to be 65% for iPSC-Heps compared to 70% for PHHs.

1.3.2 Multiplex Assays and iPSC-Heps

A series of different studies have been conducted that focus on multiplexing assays for high-throughput purposes. One study focused on utilizing various assays to analyze cytoskeletal integrity, cell viability, mitochondrial integrity, lipid accumulation, and reactive oxygen species (ROS) formation in iPSC-Heps [84]. In a separate study, Sirenko *et al.* combined three dyes to obtain readouts for cell viability (Calcein AM), mitochondrial permeability (MitoTracker Orange), and total cell number (Hoechst) to produce a general toxicity assessment [85]. This multi-parameter cellular toxicity assay was combined with the JC-10 assay, to identify specific mechanisms by which mitochondrial damage resulted in toxicity. In this study, 240 compounds were analyzed and the various assay readouts were used to rank each compound's potential hepatotoxicity. The system was able to detect toxicity for compounds in the categories of anticancer, hormonal, cardiac, anti-fungal, and anti-inflammatory drugs as well as, neuroleptics, anti-histamines, statins, and antibiotics, while also being able to rank the non-toxic compounds as such.

A similar multiplexing study was conducted on iPSC-Heps in a 3D spheroid cultured [86]. Different combinations of assay dyes that measured cellular viability, apoptosis, and mitochondrial permeability were used to characterize the spheroids. With a library of 48 different compounds known to be either hepatotoxic (e.g. Staurosporine, Paclitaxel, and Tolcapone) or non-hepatotoxic (e.g. Aspirin and Ampicillin) the iPSC-Heps cultured in 3D spheroids showed 100% specificity and 86% sensitivity when analyzed for cell viability.

1.3.3 Long-Term Toxicity Assessments

Since iPSC-Heps have been maintained in culture for up to 4 weeks [57], long term toxicity studies are now possible. Holmgren *et al.* dosed iPSC-Heps for periods of 2, 7, and 14 days and the cells exhibited greater hepatotoxicity upon longer drug exposure and a dose-dependent response to both amiodarone and aflatoxin B1 [87]. The iPSC-Hep cultures also showed signs of phospholipidosis and steatosis, but resembled similar levels of toxicity to HepG2 cells at the shorter 48 hour time point. In a study that compared PHHs iPSC-Heps, and HepaRG cultures, significant differences were observed in their gene expression [88]. PHHs expressed higher expression of genes involved in metabolism whereas genes involved in cell division and endocytosis were higher in the HepaRG and iPSC-Hep cultures. The authors reported that gene expression profiles were stable in PHHs for up to 2 weeks. Toxicants were administered for either 2, 7, or 14 days and Bell *et al.* reported that the 3D PHH spheroids exhibited the highest sensitivity to all six compounds that were tested.

1.3.4 Patient-Specific Toxicity Investigations using iPSCs

One of the advantages of using iPSC-Heps is retention of the genotype of the original donor, leading to the potential of identifying patient-specific therapeutics or disease mechanisms. Differences in CYP activities can be correlated to alterations in the genes through single nucleotide polymorphisms (SNPs) [89, 90]. Genetic differences can impact the results of comparative cellular studies since the iPSC-Heps and PHHs do not come from the same donor [89]. Takayama *et al.* were able to use 12 different PHH donors to produce iPSCs and then differentiate the cells back to a hepatocyte phenotype [89]. This generated iPSC-Heps that had the same genetic make-up as their PHH donors. CYP1A2, 2C9, and 3A4 activity levels as well as the expression of liver-specific genes and transporters detected in the iPSC-Heps correlated to the levels measured in the corresponding PHHs. The authors targeted CYP2D6 to analyze the

retention of genetic differences since this gene has a large range of functional variability, which can mostly be attributed to SNPs [89, 91]. With inter-individual CYP2D6 differences among the 12 PHH donors it was reported that these unique metabolic alterations transferred to the iPSC-Heps, establishing that such cells can be used for personalized drug screening [89].

Developing iPSC lines from patients with specific genetic disorders has been conducted for diseases such as Huntington's, Parkinson's, and muscular dystrophy [92]. This has also been done in relation to patients with liver-specific diseases, from which iPSC-Heps were generated [93]. iPSC-Heps that may retain a diseased phenotype could lead to a deeper understanding of cell signaling and function in diseased tissues. For patients with Alpers-Huttenlocher syndrome (AHS), a genetic disorder of mitochondrial DNA, there is an unexplainable development of hepatotoxicity when they are treated with VPA a common drug used to treat epilepsy [94]. Li *et al.* developed iPSC-Heps from two patients with AHS to uncover the mechanism behind the VPA induced toxicity. They discovered that genetic mutations lead to the mitochondrial permeability transition pore (mPTP) opening more frequently resulting in increased apoptosis [94]. Furthermore, an mPTP inhibitor, cyclosporine A, was able to significantly reduce apoptosis by ~15-40% when the AHS-derived iPSC-Heps were treated with VPA [94]. In another study, an iPSC cell line of homozygous familial hypercholesterolemia was differentiated to a hepatocyte phenotype to screen for potential drug treatments [95]. This disease is mainly caused by a mutation in the low-density lipoprotein receptor (LDLR), which causes increased levels of LDL-cholesterol (LDL-C) leading to cardiovascular complications. A library of 2,320 compounds was tested to identify reductions in LDL-C levels. Cayo *et al.* reported that of the 13 compounds that resulted in reproducible decreases, five were cardiac glycosides. It was determined that this family of drugs lowers LDL-C levels by promoting the degradation of apoB, a VLDL precursor [95]. The cardiac glycosides was validated with three *in vitro* models (PHHs, HepG2, and iPSC-Heps***)***, as well as with mice with humanized livers and medical records from patients. These studies

illustrate how the use of disease specific iPSC-Heps can be used to screen for potential therapeutic treatments.

1.4 Discussion and Conclusions

While the use of iPSC-Heps has proven valuable in toxicity testing there are still limitations to their utilization. Many protocols exist to differentiate iPSCs to hepatocytes and although they generally follow the same basic procedure, slight differences may yield a different cell phenotype. In a detailed computational and experimental study conducted by Salomonis *et al*., on 58 iPSCs obtained from 10 different research groups, several concerns were identified [96]. The authors reported several issues with iPSCs such as contamination, formation of teratomas, morphological and karyotypic abnormalities. The concerns raised in this study will require additional experimentation to fully understand how iPSCs may be utilized in tissue engineering and toxicity studies.

For iPSC-Heps, some of the main concerns are variations in differentiation protocols and the expressions of adult hepatocyte markers. In the absence of a consistent differentiation protocol conflicting results may be obtained. For example, Medine *et al.* observed CYP1A2 and CYP 3A activity levels at 1% and 34% of those detected in PHHs, respectively [61]. These findings are in contrast to Lu *et al.* who reported that activities for both of those enzymes fell in the upper range of PHH activity [60]. Differences were also reported between hepatocytes derived from iPSCs and ESCs with the same differentiation protocol when analyzing gene expression, urea production and albumin secretion [62].

iPSC-Heps can maintain the genetic make-up of their original source, enabling the investigations of specific genetic polymorphisms [89]. This is a very attractive and promising feature of these cells. If cells from diseased patients can be obtained then it is likely that in the future patient-

specific toxicity and therapeutics testing can be conducted [94, 95]. For these reasons, iPSC-Heps have the potential to be used for a variety of investigations, such as chronic toxicity, individualized drug screening, high-throughput testing, and mechanistic analysis [43, 77]. It is also feasible to utilize iPSCs to conduct pre-clinical screening of potential therapeutic compounds [70, 97]. In conclusion, iPSC-Heps are a promising new advancement in the area of designing engineered hepatic tissues and in liver toxicity. Future studies will continue to pave the way for iPSC-Heps in hepatotoxicity testing and in understanding of disease mechanisms.

1.5 Research Objectives

iPSC-Heps are a relatively new cell type available for *in vitro* hepatic investigations. Little information has been established regarding the functional markers of adult hepatic phenotypes. There is also a critical need to compare their functional characteristics to mature primary human hepatocytes. Currently iPSC-Heps exhibit reduced hepatic function relative to PHHs, which is hindering their utility in hepatotoxicity evaluations. We aim to improve iPSC-Hep function by developing a 3D liver model that incorporates other hepatic non-parenchymal cells. iPSC-Hep functionality will be benchmarked against PHHs since these cells are derived from liver tissue and exhibit hepatic functions that are close to those observed *in vivo*. We will administer hepatotoxicants such as acetaminophen and ethanol at different concentrations. We will conduct immunofluorescence measurements on protein expression, and measure markers of liver function and toxicity. Our goal in this thesis is to obtain a comprehensive understanding on the liver functions of iPSC-Heps cultured in 3D models.

There are three primary research objectives:

Objective I. Investigating the Function of iPSC-Heps Cultured as Monolayers or in Collagen Sandwich Cultures

Objective II. Developing 3D iPSC-Hep and Non-Parenchymal cell Model for Hepatotoxicity Testing

Objective III. Conducting RNA Sequencing of iPSC-Heps and PHHs; Future Directions

Chapter 2: Investigating the Function of iPSC-Heps Cultured as Monolayers or in Collagen Sandwich Cultures

2.1 Introduction

Induced pluripotent stem cell derived hepatocytes (iPSC-Heps) are an emerging new cell type for the use of *in vitro* hepatocyte studies. In the past studies have primarily used genetically manipulated or hepatoma cell lines and primary human hepatocytes (PHHs). Issues related to the phenotypic accuracy of cell lines have prevented them from becoming a reliable source [66, 70]. PHHs exhibit complete hepatocyte function and enzymatic activity levels [69]. While PHHs are preferred for *in vitro* studies on human liver functions, the difficulties associated with their limited availability and donor-to-donor variations poses problems [42, 67, 71, 77].

iPSC-Heps are emerging as a new class of cells that may provide comprehensive information about human hepatic function. These cells are not fully studied and there are concerns about their functions compared to PHHs [61, 78]. Differing differentiation protocols can lead to issues related to differences in their gene expression [96]. In addition there is concern that these cells are not fully mature and may exhibit markers of a fetal phenotype [45, 46]. Despite these challenges, the promise and scientific possibilities of iPSC-Heps outweigh their current drawbacks. Advancements in differentiation procedures have continued to promote the use of iPSC-Heps and demonstrate that improved hepatocyte functionality is attainable [45, 51, 54]. In this project iPSCs differentiated towards a hepatocyte phenotype were obtained from a commercial source. The iPSC-Heps were differentiated from fibroblasts from a Caucasian female donor.

Much of the past work done with iPSC-Heps have utilized the iCell Hepatocytes 1.0 version, which requires the use of a Matrigel overlay [57, 58, 60]. iCell Hepatocytes 2.0 do not require the use

of an ECM overlay, hence the investigation into utilizing collagen to form sandwich (CS) cultures. This study directly compared monolayer and CS culture models (**Figure 2.1**).

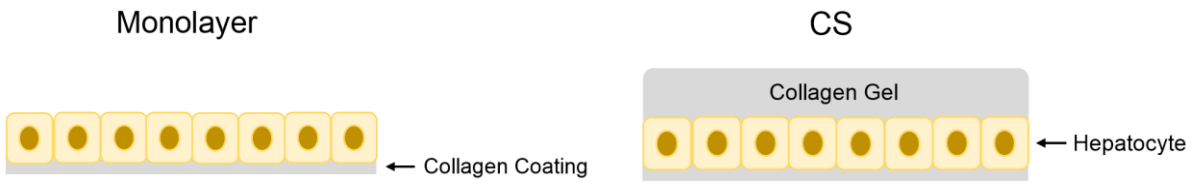

Figure 2.1: Schematic representing iPSC-Heps in monolayer and CS culture models. The iPSC-Heps are maintained as a confluent layer seeded onto a collagen coating in the monolayer model. CS model has a 1.1 mg/ml collagen gel added onto the confluent layer of cells.

Our focus is to utilize iPSC-Heps in 3D models to investigate hepatotoxicity. To achieve this goal, our first objective was to find out an optimal culture condition for these cells. The vendor from where these cells are procured provided guidelines only on culturing iPSC-Heps as monolayers. Since the assembly of a 3D liver model will require the sequential stacking of hepatocytes and non-parenchymal hepatic cells, we decided to investigate whether culturing iPSC-Heps in a sandwich culture would affect their viability and function. For this reason, we first compared the properties of iPSC-Heps cultured in monolayers and in sandwich cultures.

2.2 Materials and Methods

RPMI, B27 supplement, phosphate buffered saline (PBS), Tris-HCl, sodium acetate, acetonitrile, ethylenediaminetetraacetic acid (EDTA), ethanol, and TrypLE were obtained from Thermo Fisher Scientific (Waltham, MA). Gentamicin, collagenase, 7-methoxy-4-trifluoromethylcoumarin (MFC), 7-hydroxy-4-trifluoromethylcoumarin (HFC), sodium dodecyl sulfate (SDS), and β-glucuronidase/arylsulfatase were purchased from Sigma-Aldrich (St. Louis, MO). Oncostatin M was obtained from R&D systems (Minneapolis, MN). Dexamethasone was purchased from MP Biomedicals (Solon, OH).

2.2.1 Collagen Extraction

Type I collagen was extracted from rat tails, which has been previously described [98-100]. In summary, tendons obtained from rat tails were dissolved in acetic acid. The resulting collagen solution was purified through centrifugation at 13,000 x g and precipitated with 30% (w/v) sodium chloride. Collagen was centrifuged at 8500 x g and the dialyzed in 1 mM hydrochloric acid. The solution was sterilized with chloroform and maintained at a concentration of 2.0–3.0 mg/ml with a pH of 3.1.

2.2.2 iPSC-Hep Cell Cultures

iPSC-Heps were purchased from a commercial source (iCell Hepatocytes 2.0; Cellular Dynamics International (CDI), Madison WI). The iPSC-Heps were differentiated from fibroblasts obtained from a Caucasian female donor. Cells were received cryopreserved from CDI and were cultured as per the manufacturer's instructions. Upon thawing, the cells were plated and maintained until day 4 in manufacturer recommended plating medium. Plating medium consisted of RPMI supplemented with 20 ng/ml Oncostatin M, 0.1 µM dexamethasone, 5 µg/mL gentamicin, B27 supplement, and iCell Hepatocytes 2.0 medium supplement. On day 5 cells were then maintained in maintenance media containing RPMI, 0.1 µM dexamethasone, 5 µg/mL gentamicin, B27 supplement, and iCell Hepatocytes 2.0 medium supplement. iPSC-Heps were plated onto type I collagen-coated tissue culture polystyrene (TCPS) well-plates at a manufacturer recommended density of 300,000 cells/cm^2. Culture medium was changed every 24 hours. Cells were maintained at 37^{o}C in a humidified environment at 5% carbon dioxide.

2.2.3 Assembly of Collagen Sandwich (CS)

On day 7 of culture a 1.1 mg/ml type I collagen solution was added to the cell cultures to form a collagen gel above the monolayer of cells to form a CS culture (**Figure 2.2**). Collagen was allowed

to gel for ~45 minutes at 37ºC and then hydrated with maintenance medium. The second layer of collagen was placed on day 7 since the manufacturer recommended assaying the iCell Hepatocytes 2.0 beginning only on day 7. It is recommended to not assay the iPSC-Heps until day 7 post-plating (personal communications).

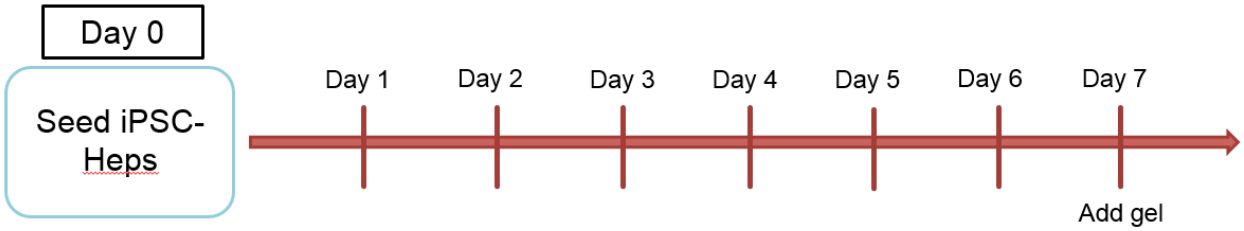

Figure 2.2: Experimental timeline. Collagen gel is added to CS samples on day 7 of culture. iPSC-Heps should not be assayed until the day 7 time point.

2.2.4 Assaying for Secreted Urea

The spent culture medium was assayed for the secretion of urea using a colorimetric BUN kit (StanBio Laboratory, Boerne, TX). The standard curve was obtained by diluting urea into the iPSC-Hep culture medium. The urea concentration was determined through absorbance measurements at 520 nm.

2.2.5 DNA Quantification

To quantify the amount of cells present in each well at day 9 and 18 of culture the cells were collected. iPSC-Heps were released from culture through the use of TrypLE. The resulting cell suspensions were collected and centrifuged at 800 x g for 2 minutes and then re-suspended in an SDS solution. The SDS solution contained 0.1% (w/v) SDS, 1 mM EDTA, and 100 mM Tris-HCl. DNA quantification of the lysate was conducted using the Quant-iT PicoGreen kit (Thermo Fisher Scientific) [58]. A standard curve was generated using the provided Lambda DNA. Aliquots of the original sample lysate solutions were diluted 10X in TE buffer prior to being assayed. Fluorescence was measured at Excitation 480/Emission 520 nm.

2.2.6 Statistical Analysis

All results are reported as mean ± standard deviation; n represents the sample size. Statistical significance was determined using a two-tailed Student's t-test with $\alpha = 0.05$. Equal variance was assumed for equal sample sizes and unequal variance was assumed for different sample sizes. The Bonferroni correction (multiple hypothesis testing) was applied.

2.3 Results

2.3.1 Cellular Morphology

As early as two days post-plating, the iPSC-Heps began to exhibit typical hepatocyte morphology. Phase contrast images show cells with a cobblestone morphology and distinct nuclei (**Figure 2.3**). The presence of binucleated cells, a characteristic of hepatocytes, was also observed in the phase contrast images. This cuboidal morphology was maintained for the entire duration of the culture. iPSC-Hep morphology was not impacted by culturing iCell Hepatocytes 2.0 in a CS culture (**Figure 2.4**). Cellular morphology was not altered by the presence of the gel, indicating that the iPSC-Heps could be cultured in this configuration.

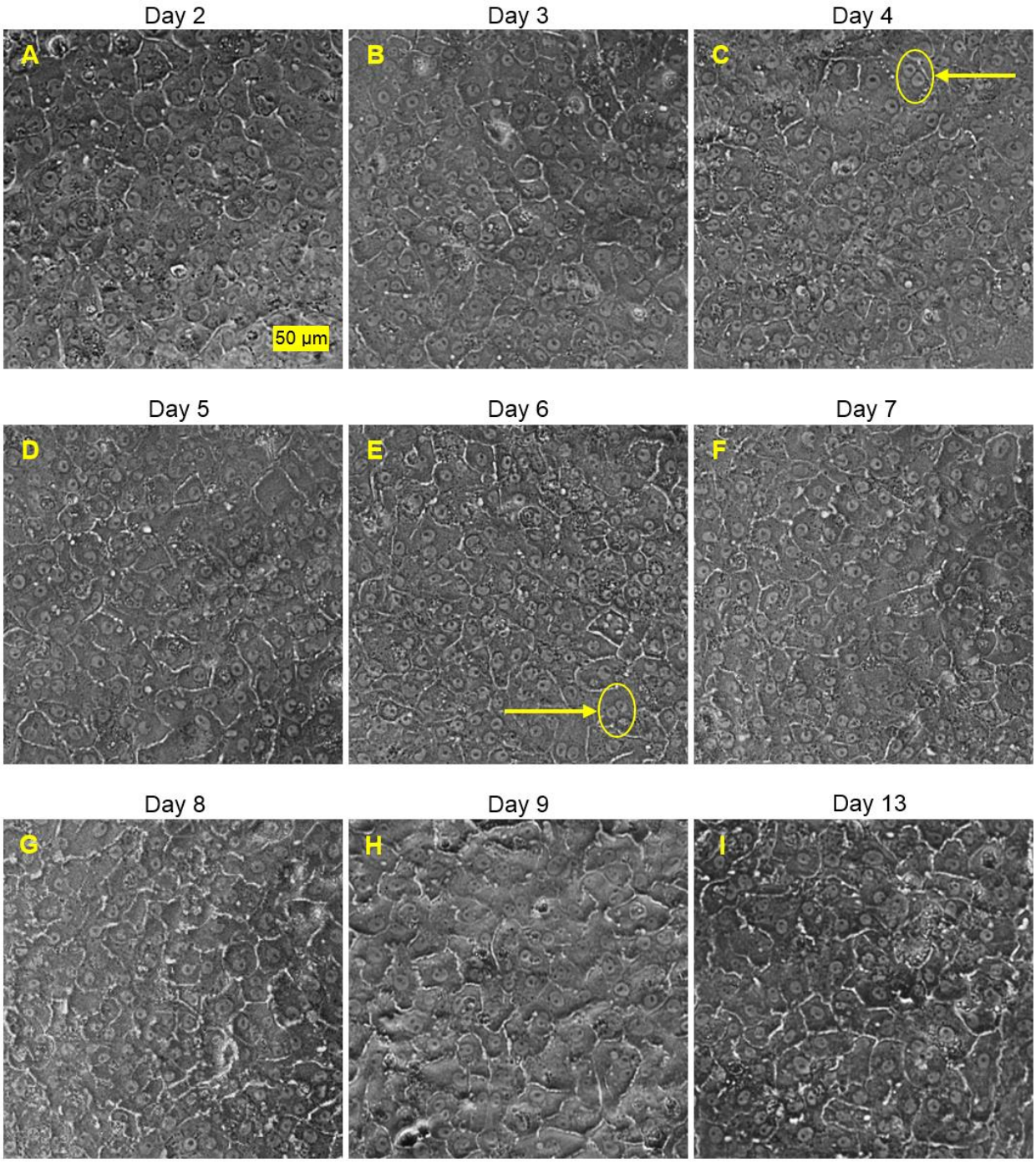

Figure 2.3: Representative phase contrast images iPSC-Heps as a monolayer over time in culture for (**A**) day 2, (**B**), day 3, (**C**), day 4, (**D**) day 5, (**E**) day 6, (**F**) day 7, (**G**) day 8, (**H**) day 9, and (**I**) day 13 (scale bar = 50 µm). Examples of binucleated cells are highlighted by yellow arrows.

iPSC-Heps in the monolayer and CS cultures were maintained up to 18 days after plating (**Figure 2.4**).

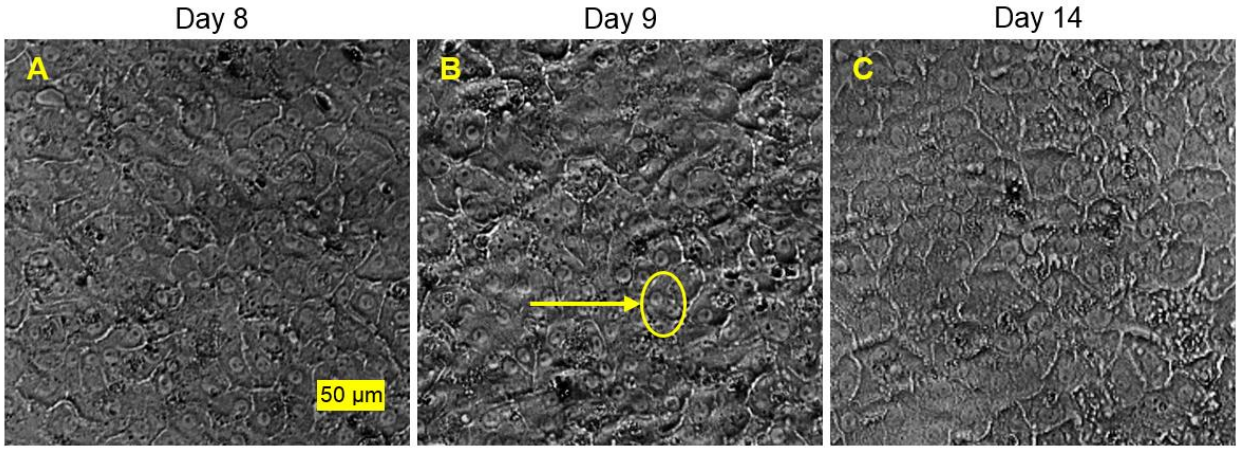

Figure 2.4: Representative phase contrast images of iPSC-Hep in the CS model over time in culture for (**A**) day 8, (**B**) day 9, and (**C**) day 14 (scale bar = 50 µm). An example of a binucleated cell is highlighted by the yellow arrow.

2.3.2 Cell Area

Individual cell areas of iPSC-Heps were measured using Nikon NIS-Elements software. Average cell areas were determined for both the monolayer and CS at the day 8 and 9 time points (**Figure 2.5**). The results show a statistically significant difference in cell area between the monolayer and CS models at each individual time point. Monolayers are also seen to increase in size from day 8 to day 9, while the cells in the CS model decrease in size from day 8 to day 9. The percent difference for each culture model between day 8 and day 9 is < 20%, indicating these differences may be due to natural biological variation. This measurement will be conducted with a higher sample size in the future to see if the trend stays the same or deviates.

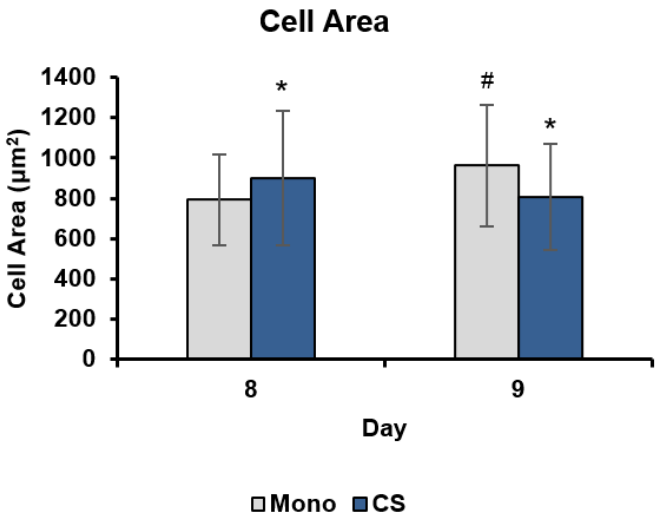

Figure 2.5: Cell areas of iPSC-Heps in the monolayer and CS models on day 8 and 9. *$p < 0.05$ between monolayer and CS at the respective time point; #$p < 0.05$ between day 8 and day 9 for each model, $n \geq 100$.

2.3.3 DNA Quantification

Cultures for both the monolayer and CS were completed on day 9 or 18 through cellular collection and lysing for DNA. There was no statistically significant difference in the final DNA values between iPSC-Hep monolayers and CS cultures at either time point (**Figure 2.6**). The CS caused no change in cellular viability. From day 9 to 18 there was a 35% decrease in DNA values in the monolayer cultures. The CS model exhibited only a 17% decrease in DNA from day 9 to 18. These trends indicate that culturing iPSC-Heps in CS cultures prevented cell death over the 18-day period.

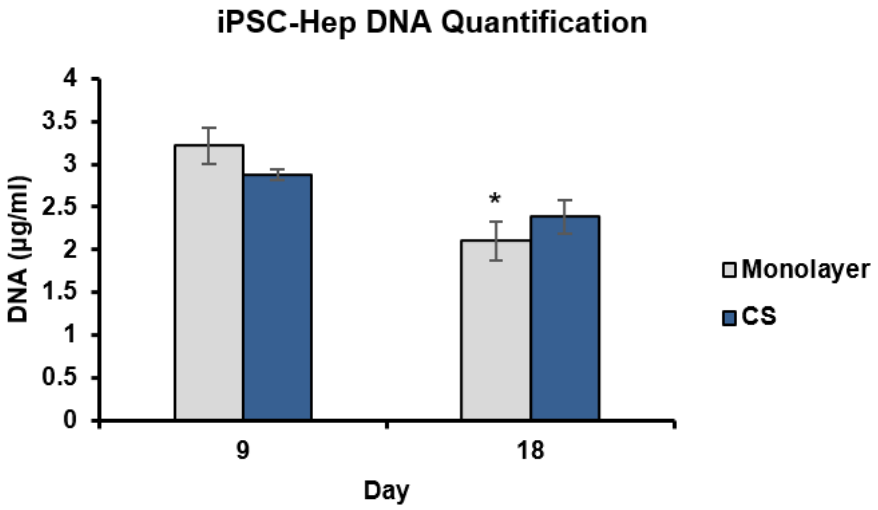

Figure 2.6: DNA quantification from monolayer and CS cultures. Cultures were ended on either day 9 or 18. Value of DNA corresponds to relative amount of cells per culture. #$p < 0.05$ for comparison between monolayer and CS models at each relative time point, *$p < 0.05$ comparison between time points for each individual model, $n = 3$.

2.3.4 Urea Secretion

To assess whether any functional differences occurred with the addition of the top gel, urea secretion was measured in spent cell culture media. Urea was measured for both cultures over the 18-day culture period to evaluate whether the addition of a second gel on day 7 changed this hepatocyte-specific marker. Since the second layer of the gel was placed on day 7 in culture, we began measuring urea secretion from day 7 onward. iPSC-Heps did exhibit the ability to secrete urea prior to day 7, beginning as early as day 2 in culture (data not shown). In the CS culture from day 7 to 8 there is only a 5.1% change in the urea secretion, indicating that the addition of the top gel did not functionally impact the iPSC-Heps (**Figure 2.7**). Analyzing urea production over time the iPSC-Heps appear to be stable in both culture models, although the CS model had a statistically significant increase in urea production between day 8 and day 18. For the monolayer cultures there was an 11% decrease in urea secretion from day 8 to day 18, while the CS actually exhibited an 85% increase in urea production between these two time points. This may indicate that the addition of the CS gel is beneficial to maintaining iPSC-Hep functionality.

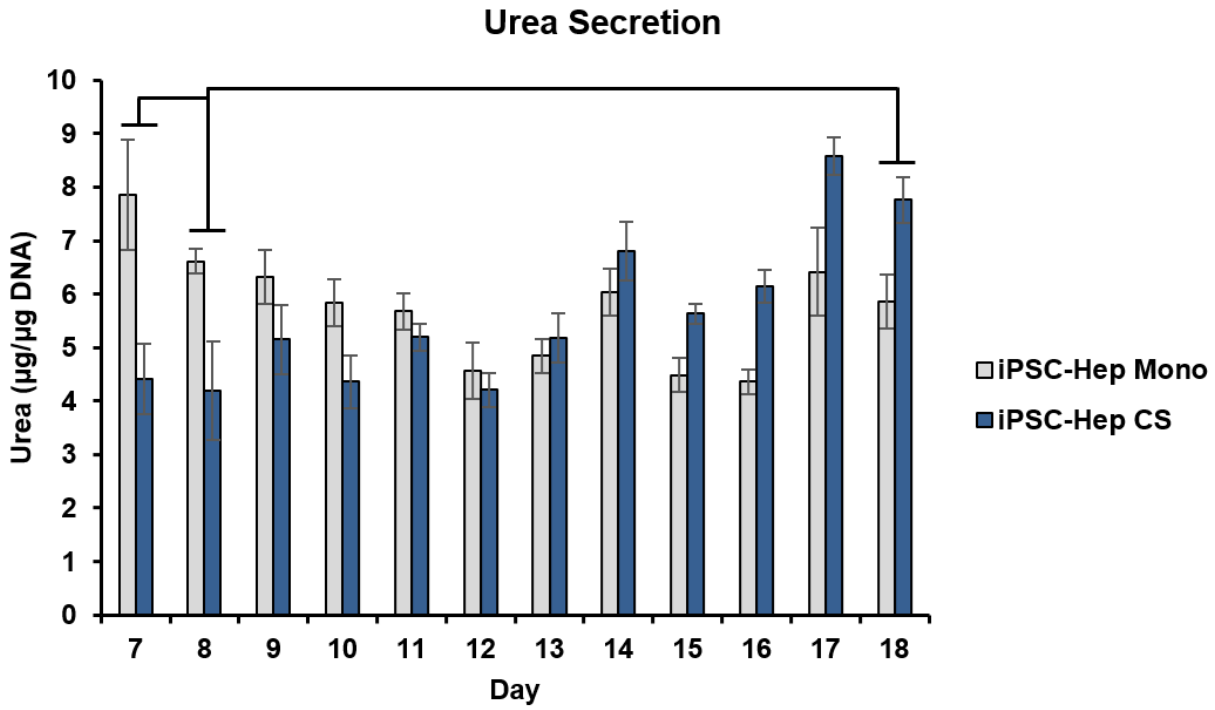

Figure 2.7: Changes in daily urea secretion was measured with spent media. Urea secretion is a marker of hepatocyte function and was measured for iPSC-Heps in the monolayer and CS models from day 7 to day 18 of culture. Comparisons were made between day 7 and day 8, as well as day 8 to day 18 for each individual model, $n = 3$.

2.4 Discussion

The main objective of this study was to determine if iCell Hepatocytes 2.0 could be successfully cultured with the addition of a collagen gel to form CS cultures. A sandwich culture is a standard model commonly used with hepatocyte cultures, as the original line of iCell Hepatocytes required the use of a Matrigel overlay [57, 60]. The iPSC-Heps were monitored up until day 18 in culture, regarding their morphology and hepatocyte function to assess any potential adverse effect of the collagen gel. Overall, our results led to the conclusion that the formation of the CS model at day 7 did not negatively impact the morphology or functionality of the iPSC-Heps over time in culture.

Cellular morphology remained unchanged between the monolayer and CS cultures, as evidenced by the phase contrast images. The iPSC-Heps maintained a polygonal morphology, indicating

visually there was no adverse reaction to the change in environment. DNA quantification from collected cell lysates revealed no statistically significant difference in the relative number of cells between the monolayer and CS models at various time points. However, there was a significant decrease in the quantity of DNA in the monolayer cultures from day 9 to day 18, demonstrating cell loss over time. Therefore, the CS exceeded the performance of the monolayer model in terms of maintaining cell attachment and culture confluency.

Urea secretion was measured as a marker of hepatocyte function to determine if the collagen gel resulted in any phenotypic changes. Analyzing the urea values for the CS cultures at day 7 and day 8, directly prior to and 24 hours after the gel addition, resulted in no significant change in urea secretion. The CS model exhibited a statistically significant increase in urea production from the beginning of CS formation (day 8) to the completion of the culture on day 18. The formation of the CS culture appears to be improving the functionality of the iPSC-Heps, as opposed to the monolayer model, when maintained in culture over time.

The results show no loss of morphology, decrease in culture viability, or reduction in functionality when comparing monolayers to the CS. The results confirm that iPSC-Heps can be cultured as CS models while maintaining cellular health over time in culture. This conclusion is promising as the collagen gel provides a platform from which to develop a 3D model. This leads to the possibility of modifying the collagen gel to assemble 3D liver models that incorporate hepatic non-parenchymal cells. iPSC-Heps have been shown to exhibit decreased function when compared to PHHs. The introduction of additional primary hepatic-specific cell types in a 3D model representative of the *in vivo* environment may improve iPSC-Hep function relative to PHHs.

Chapter 3: Developing 3D iPSC-Hep and Non-Parenchymal cell Model for Hepatotoxicity Testing

3.1 Introduction

Induced pluripotent stem cells (iPSCs) can be differentiated into multiple cell types in the body. Human iPSC-derived hepatocyte-like cells are a new source for hepatic cells. iPSC-derived hepatocyte-like cells are being evaluated on their expression of mature hepatic phenotypes and their functional capability. Since iPSC-Heps can exhibit fetal characteristics, we have assembled 3D human liver models using iPSC-Heps and hepatic non-parenchymal cells (NPCs). We have assembled similar 3D models with primary human hepatocytes to compare the functional capability of these cultures.

The liver plays an integral role in metabolism, protein synthesis and in numerous physiological functions [40, 41, 101, 102]. The principal or parenchymal cells of the liver are hepatocytes that comprise about 80% of the liver mass [42]. Hepatocytes have a polar phenotype in which there are specialized sections of the plasma membrane that enable the uni-directional absorption and secretion [103]. Absorption of nutrients and compounds from the blood passing through the sinusoids occurs at the basolateral membrane where the microvilli are located [103, 104]. Once further metabolized, the compounds are excreted to the bile duct through the apical membrane [103, 104]. In addition to hepatocytes the other primary cell types are liver sinusoidal endothelial cells (LSECs), Kupffer cells, and hepatic stellate cells (HSCs) [40, 41]. LSECs line the sinusoid, exhibit fenestrae and lack a basement membrane, which allows blood in the sinusoid to reach the hepatocytes [40, 103, 105]. Kupffer cells are the resident macrophages of the liver [40, 103, 106]. HSCs reside in the Space of Disse which lies between the hepatocytes and LSECs; they help maintain the composition of the extracellular matrix (ECM) and store vitamin A when quiescent [40, 42, 104, 107].

To fully recapitulate liver function, additional hepatic NPCs should be incorporated into *in vitro* models to better mimic the architecture of liver tissue. Some 3D primary human hepatocyte (PHH) *in vitro* models do exist that utilize hepatic NPCs such as spheroids, bioprinted tissues, and microfluidic devices [108-110]. Spheroids are globular aggregates of cells that retain a 3D structure in culture, and various groups developed co-culture spheroids of primary hepatocytes and hepatic NPCs [108, 111-113]. Bioprinted liver tissues have utilized the individual microextrusion of hepatocytes and NPCs to form distinct cellular compartments [109]. A two chamber microfluidic model has also been designed to mimic the liver sinusoid as it incorporated PHHs, and various human cell lines were used to represent LSECs, HSCs, and Kupffer cells [110]. Another model that utilized PHHs and NPCs was assembled using automated procedures to adapt the process for high-throughput toxicity screening [114].

Different models have also been developed with iPSC-Heps in order to obtain a mature hepatic phenotype. Berger *et al.* cultured iPSC-Heps in a micro-patterned co-culture model (MPCC), which involved the use of collagen-coated islands surrounded by murine fibroblasts [57]. Other models have utilized decellularized rat liver extracellular matrix (ECM) and 3D printed PLLA-collagen coated scaffolds [58]. Both studies have succeed in yielding increased iPSC-Hep function, but have still not quite reached levels as found in PHHs. None of the existing iPSC-Hep models have included hepatic NPCs. Due to the lack of *in vitro* iPSC-Hep models that generate a 3D environment and better represent the cellular composition of the liver, we have designed a 3D model that is comprised of iPSC-Heps and LSECs.

iPSC-Heps are a relatively new cell type, as the reprogramming method to generate human iPSCs was only first developed in 2007, so the extent of their hepatic capabilities are still largely unknown [10]. The ideal cell type used for hepatotoxicity testing is primary human hepatocytes (PHHs) [67,

71, 72]. PHHs are isolated from human liver tissue and contain key liver functions as well as drug metabolizing capabilities [42, 69]. However, PHHs are a limited resource and have high variability due to donor differences [42]. iPSC-Heps are being investigated as an alternative to PHHs in the area of the hepatotoxicity testing, but very few studies have extensively compared iPSC-Heps to PHHs.

Several hepatocyte markers have been identified in iPSC-Heps such as CYP activity, urea secretion, albumin production, glycogen storage, and bile canaliculi formation [57, 60-62]. Many of these markers are expressed at a lower level compared to PHHs, showing that the iPSC-Heps are not quite at the enzymatic capability of PHHs. Many baseline comparisons have been made between iPSC-Heps and PHHs that focus on particular gene expression levels and CYP activity [57, 60, 78, 80, 88]. While these primary comparisons have been done, iPSC-Heps have not been thoroughly characterized against PHHs, particularly in the area of hepatotoxic response. Many toxicity studies conducted that compare iPSC-Heps and PHHs have primarily analyzed cell viability [61, 88]. In addition to the viability measurement some reports have also included lactate dehydrogenase (LDH) release, glutathione, caspase 3/7 activity, urea secretion and albumin secretion [60, 78, 79]. To the best of our knowledge, only one report has extensively compared iPSC-Hep and PHH toxicity response through the measurements of mitochondrial membrane potential, calcium influx, oxidative stress and CYP activity among others [62].

iPSC-Heps are of particular interest for the application of hepatotoxicity studies due to the high clinical trial failure rate of potential therapeutics, with only about 11% of compounds succeeding in obtaining government approval [115]. Inadequate screening has also resulted in drugs being pulled from the market, with drug-induced liver injury (DILI) being the most common cause for post-market withdrawal [116]. Of the drugs able to remain on the market, ~10% receive black box warnings indicating a potential severe health risk [68]. So much failure is costly for the

pharmaceutical industry in terms of both time and monetary consumption. On average it costs around $1.2 billion and requires almost 9 years to complete clinical trials to bring a drug to market [117].

The objective of this study is to develop a 3D hepatocyte-LSEC culture (3DHL) to better represent the *in vivo* liver environment. The presence of another hepatic cell type should help induce a more mature hepatic phenotype in the iPSC-Heps. We will build the models for both iPSC-Heps and PHHs to directly compare functionality and how the presence of the LSECs directly impacts both cell types. We aim to administer well-studied hepatotoxicants and investigate the hepatotoxic response 24 hours after administration. This study analyzes the hepatocellular response through urea secretion, depletion of glutathione, mitochondrial membrane integrity, and CYP2E1 activity. Various toxicity markers are being investigated to obtain a more holistic analysis of the iPSC-Hep response and the impact of LSEC addition, in comparison to a traditional collagen sandwich (CS) model.

3.2 Materials and Methods

RPMI, B27 supplement, fibronectin, fetal bovine serum (FBS), Penicillin-Streptomycin, L-Glutamine, phosphate buffered saline (PBS), goat serum, sodium borohydride, bovine serum albumin (BSA), Tris-HCl, Triton X-100, sodium acetate, acetonitrile, ethylenediaminetetraacetic acid (EDTA), ethanol (EtOH), and TrypLE were obtained from Thermo Fisher Scientific (Waltham, MA). Gentamicin, endothelial cell growth supplement (ECGS), acetaminophen (APAP), glutaraldehyde, collagenase, 7-methoxy-4-trifluoromethylcoumarin (MFC), 7-hydroxy-4-trifluoromethylcoumarin (HFC), sodium dodecyl sulfate (SDS), and β-glucuronidase/arylsulfatase were purchased from Sigma-Aldrich (St. Louis, MO). Oncostatin M was obtained from R&D systems (Minneapolis, MN). Dexamethasone was purchased from MP Biomedicals (Solon, OH).

3.2.1 Collagen Extraction

Type I collagen was extracted from rat tails, which has been previously described [98-100]. In summary, tendons obtained from rat tails were dissolved in acetic acid. The resulting collagen solution was purified through centrifugation at 13,000 x g and precipitated with 30% (w/v) sodium chloride. Collagen was centrifuged at 8500 x g and the dialyzed in 1 mM hydrochloric acid. The solution was sterilized with chloroform and maintained at a concentration of 2.0–3.0 mg/ml with a pH of 3.1.

3.2.2 iPSC-Hep Cell Cultures

iPSC-Heps were purchased from a commercial source (iCell Hepatocytes 2.0; Cellular Dynamics International (CDI), Madison WI). The iPSC-Heps were differentiated from fibroblasts obtained from a Caucasian female donor. Cells were received cryopreserved from CDI and were cultured as per the manufacturer's instructions. Upon thawing the cells were plated and maintained until day 4 in manufacturer recommended plating media. Plating media consisted of RPMI supplemented with 20 ng/ml Oncostatin M, 0.1 µM dexamethasone, 5 µg/mL gentamicin, B27 supplement, and iCell Hepatocytes 2.0 medium supplement. On day 5 cells were then maintained in maintenance media containing RPMI, 0.1 µM dexamethasone, 5 µg/mL gentamicin, B27 supplement, and iCell Hepatocytes 2.0 medium supplement.

3.2.3 Primary Human Hepatocyte Cultures

PHHs were obtained from Sekisui XenoTech, LLC (Kansas City, KS). The PHH donor was a 26 year old Caucasian male with a BMI of 26.1 and no known diseases. Cells were received cryopreserved. After thawing and resuspension the cells were originally plated in manufacturer supplied OptiThaw media. The cells were further maintained in manufacturer supplied OptiCulture media.

3.2.4 Liver Sinusoidal Endothelial Cells

Human LSECs were purchased from ScienCell Research Laboratories (Carlsbad, CA). The cells were cultured onto fibronectin-coated flasks and maintained in Medium 199 supplemented with 10% FBS, 100 U/ml penicillin-streptomycin, 2 mM L-glutamine, and 12.5 ng/ml endothelial cell growth supplement. Cells were only used under a passage number of 5.

3.2.5 Culturing Conditions

iPSC-Heps were plated onto type I collagen-coated tissue culture polystyrene (TCPS) well-plates at a manufacturer recommended density of 300,000 cells/cm^2. PHHs were plated onto 1.1 mg/ml type I collagen gels at a concentration of 35,000 cells/well for a 96-well plate. Plating number of PHHs was based upon previously optimized cell densities [114]. The cell concentration for PHHs was scaled linearly for larger well plate sizes. Culture medium was changed every 24 hours for both cell cultures. Cell cultures were maintained at 37ºC in a humidified environment at 5% carbon dioxide.

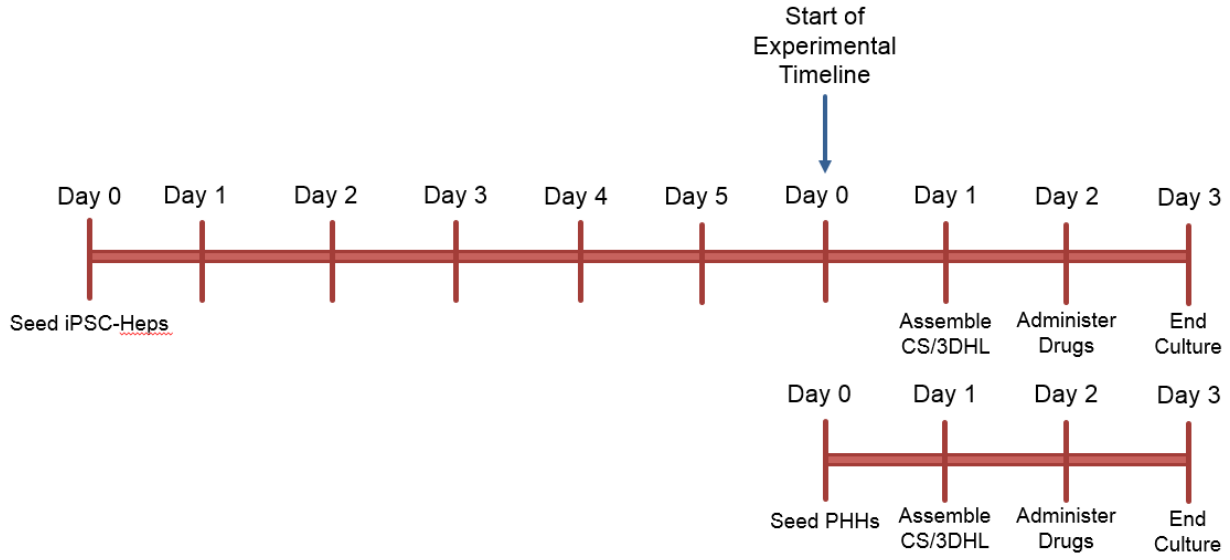

Figure 3.1: Layout of culture timeline. iPSC-Heps are seeded 6 days prior to the seeding of the PHHs. This is done to align the time points when each cell type can be used for assay. The experimental timeline designates day 0 as when the PHHs are seeded. 24 hours after the PHHs are seeded the CS and 3DHL cultures are assembled. 24 hours after assembly toxicants are administered. All of the cultures are ended 24 hours after drug administration.

For use of the iCell Hepatocytes 2.0 the company does not recommend assaying the cells until day 7 (personal communication). Past publications involving the use of iCell Hepatocytes 2.0 have allowed the cells to incubate for 8 days prior to the addition of chemical compounds [84]. The PHHs can be used for assay 24 hours after plating. The PHHs were plated 6 days after the seeding of the iPSC-Heps to align the timeline of the two cell types (**Figure 3.1**). The results are based upon the time line of thawing the PHHs as Day 0.

3.2.6 Assembly of Collagen Sandwich (CS) and 3DHL Cultures

24 hours after the seeding of the PHHs a 1.1 mg/ml type I collagen solution was added to the cell cultures to form a collagen gel above the monolayer of cells to form a CS culture (**Figure 3.2**). Collagen was allowed to form for ~45 minutes at 37ºC and then was hydrated with the respective hepatocyte medium. LSECs were re-suspended in a type I collagen solution containing 1% (v/v) fibronectin and added to the cell cultures to form the 3DHL model (**Figure 3.2**). The encapsulated LSECs were seeded at a ratio of 5:1 (hepatocytes:LSECs). The ratio was chosen based upon the cellular ratios found *in vivo* in the liver [40, 114, 118].

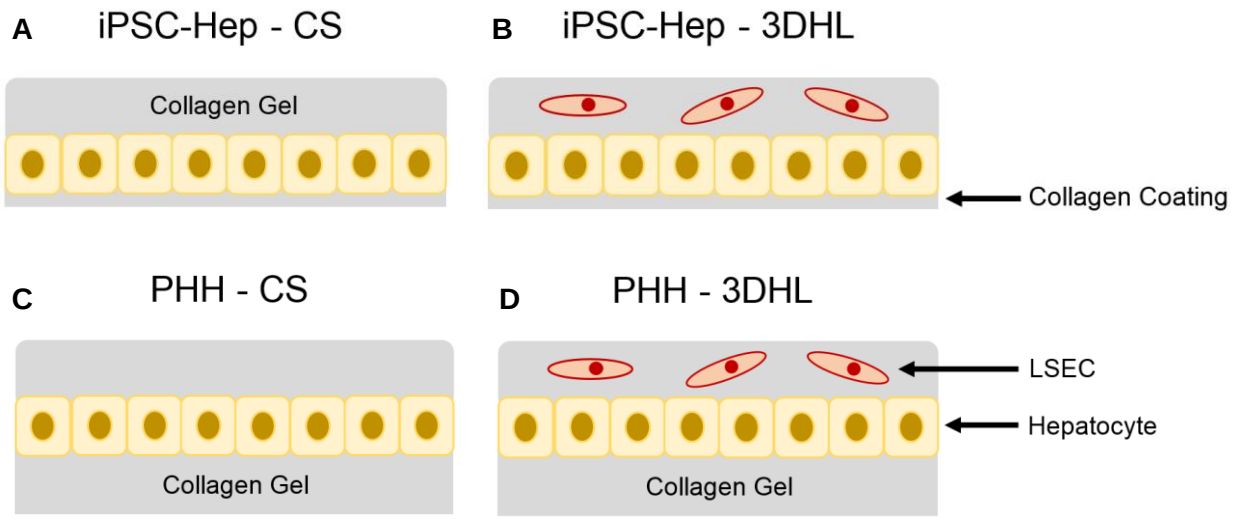

Figure 3.2: Schematics representing the various culture models for (**A, B**) iPSC-Heps and (**C, D**) PHHs. The iPSC-Hep cultures are seeded on top of a collagen coating, while the PHHs are seeded onto a collagen gel. The (**A, C**) CS cultures have a collagen gel added above the hepatocytes, while the (**B, D**) 3DHL cultures have LSECs encapsulated in the top collagen gel.

3.2.7 Addition of Toxicants

24 hours after the addition of the top gels to form the final CS and 3DHL models, toxicants were dissolved individually in either iPSC-Hep media or PHH media. Acetaminophen (APAP) was added at 2.5 mM and 5 mM, which corresponds to human LC_{50} and 2 x LC_{50}, respectively [65, 119]. LC_{50} is the concentration that causes 50% cell death [119]. Ethanol (EtOH) was added at concentrations of 80 mM and 160 mM, which is the human ½ LC_{50} and LC_{50}, respectively [65, 119].

3.2.8 Imaging Phenotypes of Hepatic Cells

Cells were fixed in a 2% (v/v) glutaraldehyde solution in PBS. The cells were then exposed to a 0.1% (w/v) sodium borohydride solution and 0.1% (v/v) Triton-X 100 solution in that respective order, both solutions were dissolved or diluted in PBS. A 1.5% (v/v) goat serum was made with a 1% (w/v) BSA solution and added to the cultures as a blocking solution. Hepatocellular albumin production was identified with a sheep serum albumin antibody (Abcam, Cambridge, MA) at a dilution of 1:100 and a donkey DAPI-conjugated secondary antibody (Thermo Fisher Scientific) at a dilution of 1:500. Bile canaliculi were identified with a mouse CD26 antibody (Thermo Fisher Scientific) at a dilution of 1:20 and a rabbit TRITC-conjugated secondary antibody (Abcam) at a dilution of 1:2000. LSECs were identified with a mouse sinusoidal endothelial-1 antibody (Novus Biologicals, Littleton, CO) at a dilution of 1:200 and the aforementioned TRITC mouse secondary antibody. Actin was identified with rhodamine phalloidin (Thermo Fisher Scientific) at a dilution of 1:60. Imaging was completed on a Zeiss LSM confocal microscope.

3.2.9 Assaying for Secreted Urea

The spent culture medium was assayed for the secretion of urea using a colorimetric BUN kit (StanBio Laboratory, Boerne, TX). The standard curve was developed by diluting urea into the respective iPSC-Hep and PHH mediums. The urea concentration was determined through absorbance measurements at 520 nm.

3.2.10 DNA Quantification

To quantify the amount of cells present in each well at day 3 of culture the cells were collected. iPSC-Heps were released from culture through use of TrypLE. Collagenase was added to PHH cultures to breakdown the surrounding collagen gels. 3DHL cultures were digested with collagenase and then the LSECs were removed from the cell suspension through the use of SE-1 coated Dynabeads ® as a part of the CELLection Pan Mouse IgG kit (Thermo Fisher Scientific). The resulting cell suspensions were collected, pelleted at 800 g for 2 minutes and then re-suspended in an SDS solution. The SDS solution contained 0.1% (w/v) SDS, 1 mM EDTA, and 100 mM Tris-HCl. DNA quantification of the lysate was completed using the Quant-iT PicoGreen kit (Thermo Fisher Scientific). A standard curve was generated using the provided Lambda DNA. Aliquots of the original sample lysate solutions were diluted 10X in TE buffer prior to being assayed. Fluorescence was measured at Excitation 480/Emission 520 nm.

3.2.11 Cytochrome P450 Activities

24 hours after toxicants were administered CYP activity of CYP2E1 was measured using a previously optimized and established protocol [114, 120, 121]. Enzymatic activity was measured through the metabolic conversion of fluorogenic substrates. For CYP2E1 MFC was converted to HFC. 10 μM of MFC was added to the cultures and allowed to incubate at 37ºC for 60 minutes. The culture medium was collected and combined with a 1:100 dilution of β-glucuronidase/arylsulfatase in DI water and a 0.5 M acetic acid solution (pH 4.5). The mixture incubated at 37ºC for 2 hours. An equivalent volume of a quenching solution containing 0.25 M Tris in 60% (v/v) acetonitrile was added to stop the reaction. The resulting HFC concentrations were determined by measuring the fluorescence at Ex410/Em510 nm. A standard HFC curve was developed to correlate the HFC concentrations to the CYP enzyme activity.

3.2.12 Quantification of Glutathione (GSH)

24 hours after chemical treatment the cultures were assayed for glutathione using the GSH-Glo assay (Promega, Madison, WI). The GSH-Glo reagent containing the Luciferin-NT substrate and Glutathione S-Transferase was added to the cultures to incubate for 30 minutes at room temperature. Luciferin detection reagent was then added to generate a luminescent signal. The luminescence was measured and treated samples were compared to the controls to quantify the differences in glutathione.

3.2.13 Analyzing Mitochondrial Membrane Integrity

After 24 hours of toxicant administration the mitochondrial membrane integrity was measured using the JC-1 Mitochondrial Membrane Potential Detection Kit (Biotium). JC-1 cationic dye (5,5',6,6'-tetrachloro-1,1',3,3'-tetraethylbenzimidazolylcarbocyanine iodide) was added to the cell cultures and allowed to incubate for 15 minutes at 37ºC. The fluorescence was measured to determine the amount of both healthy (red; Ex550/Em600) and damaged (green; Ex485/Em535) cells. The ratio of red to green determined changes in the mitochondrial membrane integrity, with decreased ratios indicating mitochondrial damage.

3.2.14 Statistical Analysis

All results are reported as mean ± standard deviation; n represents the sample size. Statistical significance was determined using a two-tailed Student's t-test with $\alpha = 0.05$. Equal variance was assumed for equal sample sizes and unequal variance was assumed for different sample sizes. The Bonferroni correction (multiple hypothesis testing) was applied.

3.3 Results

3.3.1 Measuring Changes in iPSC-Hep Cellular Morphology

iPSC-Heps closely resembled the morphology of PHHs and maintained this morphology for the duration of the culture. The iPSC-Heps exhibited a cobblestone morphology and a distinct

nucleus (**Figure 3.3**). Binucleated cells were present in both the iPSC-Heps and PHHs. Over the course of the culturing period the cells maintained viability and showed minimal morphologic changes over time.

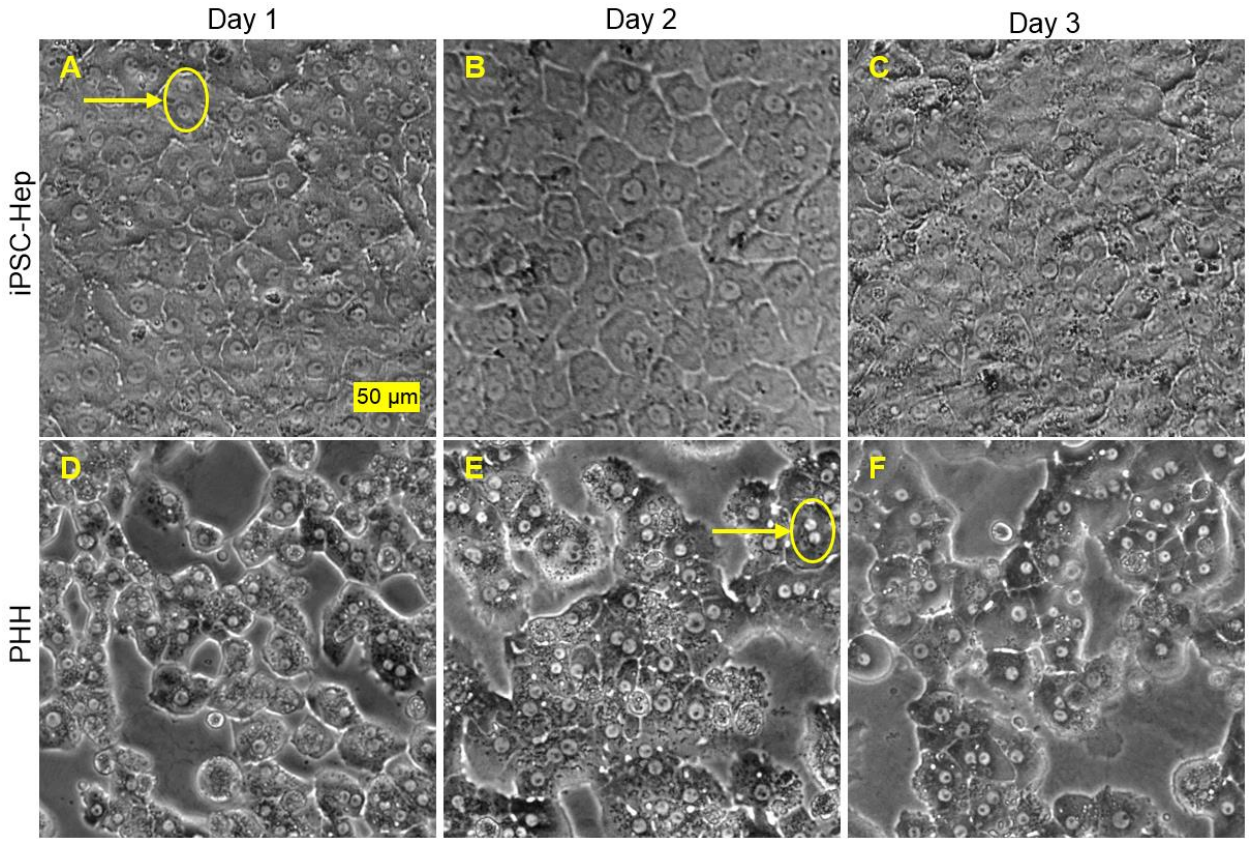

Figure 3.3: Representative images of (**A-C**) iPSC-Heps and (**D-F**) PHHs over time in culture as CS models. The images for Day 1 are prior to gel addition. Examples of binucleated cells are highlighted by the yellow arrows. Scale bar = 50 µm.

3.3.2 Comparison of Cell Areas between iPSC-Heps and PHHs in a CS Culture

Individual cell areas of iPSC-Heps and PHHs in CS cultures were measured using Nikon NIS-Elements software at day 2 and 3 of culture. At day 2 the average cell area for iPSC-Heps and PHHs was 903 ± 333 and 1496 ± 474 µm^2, respectively. The average cell areas at day 3 were 807 ± 262 µm^2 for iPSC-Heps and 1221 ± 353 µm^2 for PHHs. At both time points the PHHs exhibited a significantly larger cell area than the iPSC-Heps ($p < 0.05$). Over time in culture the iPSC-Heps did not change in size in the CS model. The PHHs did show a statistically significant

decrease in cell area from day 2 to 3. On average the PHHs exhibited 40-49% difference in cell area in comparison to the iPSC-Heps.

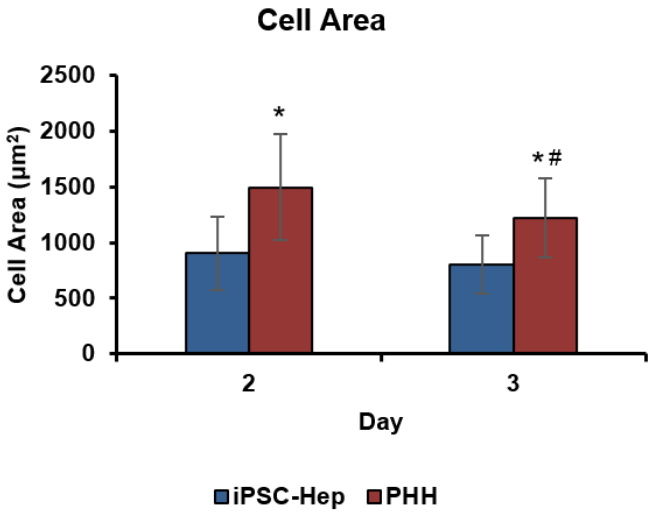

Figure 3.4: Cell areas of iPSC-Heps and PHHs in CS cultures on day 2 and 3. *p < 0.05 relative to the iPSC-Hep value at each respective time point; #p < 0.05 relative to the day 2 value for each respective model, n ≥ 100.

3.3.3 Measuring Urea Secretion and Investigating the Effect of Adding LSECs

To understand differences in baseline hepatocyte functionality, urea secretion was measured for both iPSC-Heps and PHHs as a CS model on days 2 and 3. Urea secretion was normalized to DNA. On day 2 the urea secretion for iPSC-Heps and PHHs was 2.92 ± 0.286 and 7.5 ± 0.374 µg/µg DNA, respectively. On day 3 the urea secretion for iPSC-Heps was 3.20 ± 0.145 µg/µg DNA while the PHHs was 6.5 ± 0.963 µg/µg DNA. PHH urea secretion was ~2 - 2.5 fold higher than the iPSC-Hep urea secretion for both days (**Figure 3.5**). Neither the iPSC-Heps nor the PHHs exhibited a statistically significant change in urea secretion between day 2 and 3, indicating that the cultures were stable during this time period.

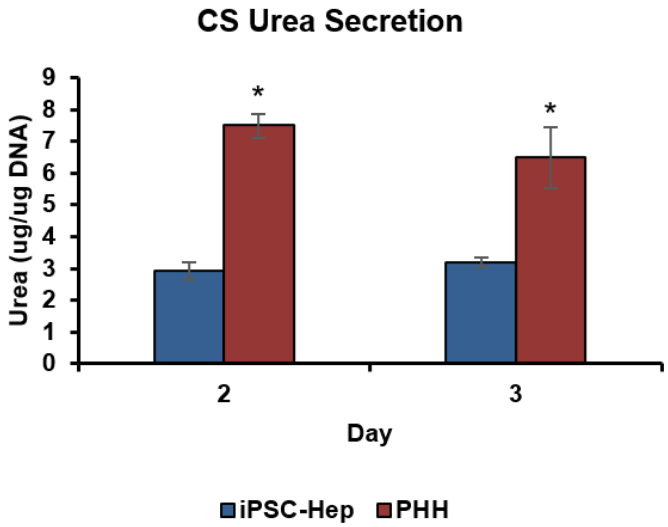

Figure 3.5: Urea secretion of iPSC-Heps and PHHs in CS model for days 2 and 3 of the control samples. *$p < 0.05$ relative to the iPSC-Hep values at each respective time point, $n \geq 3$.

In the 3DHL models the baseline urea secretion was measured and compared to their CS counterparts. At day 2 in culture the iPSC-Hep and PHH 3DHL urea secretion was 3.48 ± 0.188 and 14.0 ± 2.47 µg/µg DNA, respectively. The 3DHL models for both the iPSC-Heps and PHHs showed no statistically significant decrease from day 2 to 3 indicating cellular stability in this culture model over time. The iPSC-Heps exhibited no statistically significant increase in urea production in the 3DHL model when compared to the CS culture (**Figure 3.6A**). The PHH 3DHL cultures exhibited an increase of 86% in urea at the day 2 time point over the CS model, suggesting that adding the LSECs was beneficial for urea production (**Figure 3.6B**).

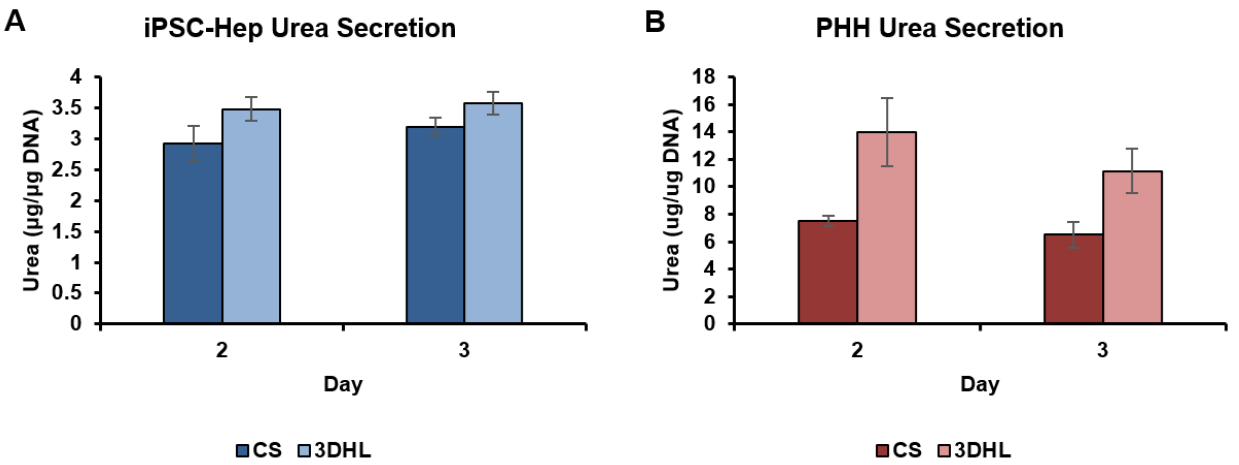

Figure 3.6: Urea secretion for (**A**) iPSC-Heps and (**B**) PHHs in the CS and 3DHL models for days 2 and 3. Day 2 is 24 hours after top gel and LSEC addition. *$p < 0.05$ relative to the CS values at each respective time point; #$p < 0.05$ relative to the day 2 value for each respective model, $n \geq 3$.

3.3.4 Immunofluorescence Imaging for Actin Cytoskeleton, Bile Canaliculi, and Intracellular Albumin

On day 3 in culture, the actin cytoskeleton was very well defined across the cross-section of iPSC-Heps in CS and 3DHL models (**Figure 3.7 A and B**). There was a distinct difference from the iPSC-Heps and PHHs. The PHHs expressed actin only in their peripheral regions, which is similar to what previous studies have reported [122]. The 3DHL model does not appear to impact the actin formation in the PHHs either.

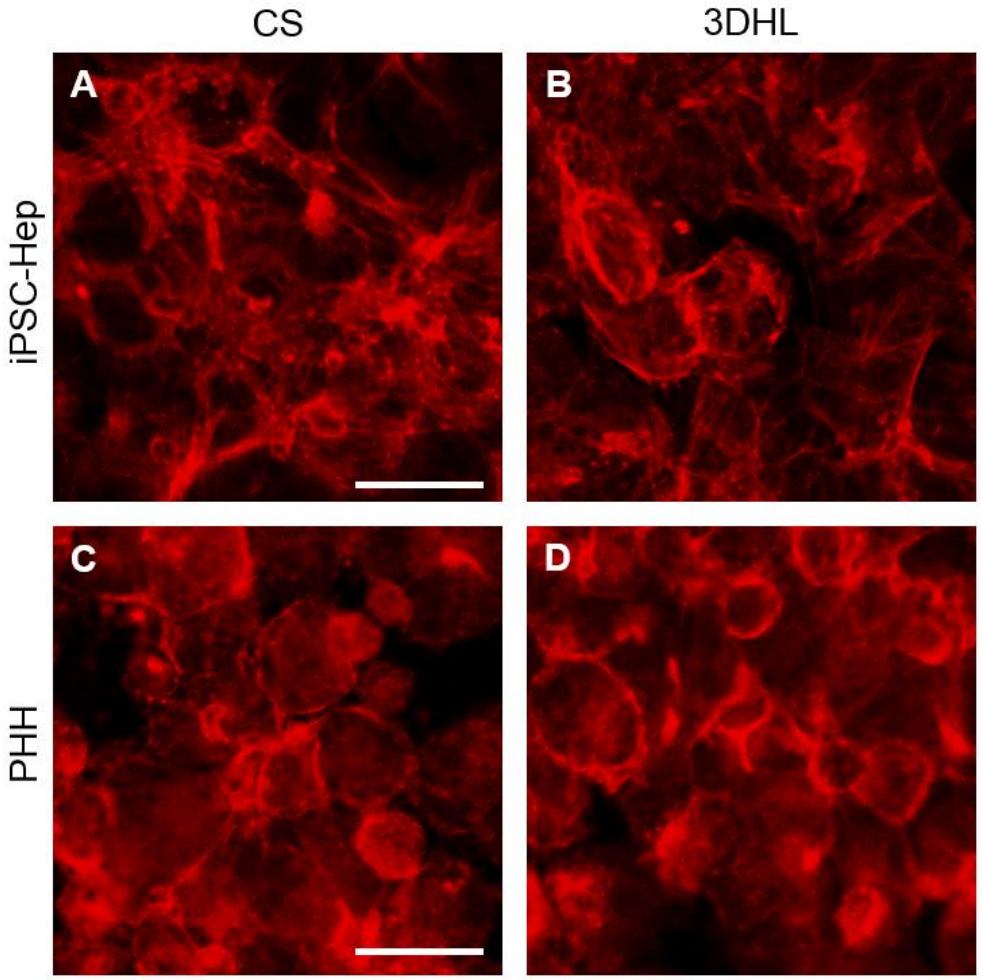

Figure 3.7: Representative images of actin cytoskeletal organization on day 3 in (**A, B**) iPSC-Hep and (**C, D**) PHH cell models (scale bars = 40 µm). Immunostaining was completed for both (**A, C**) CS and (**B, D**) 3DHL cultures.

Bile canaliculi channels are a specialized hepatic structure through which hepatocytes can excrete metabolized compounds [103]. The presence of these channels indicate maintenance of hepatocyte polarity and phenotype. Bile canaliculi formation does not appear to be present in the iPSC-Heps for either the CS or 3DHL models at the day 3 time point (**Figure 3.8 A and B**). So the addition of the LSECs do not seem to be improving iPSC-Hep polarity. Both PHH models show evidence of bile canaliculi formation (**Figure 3.8 C and D**). Retention of bile canaliculi in primary rat hepatocyte CS cultures has previously been reported [122, 123]. The presence of bile canaliculi is evidence the PHHs retain a polar phenotype.

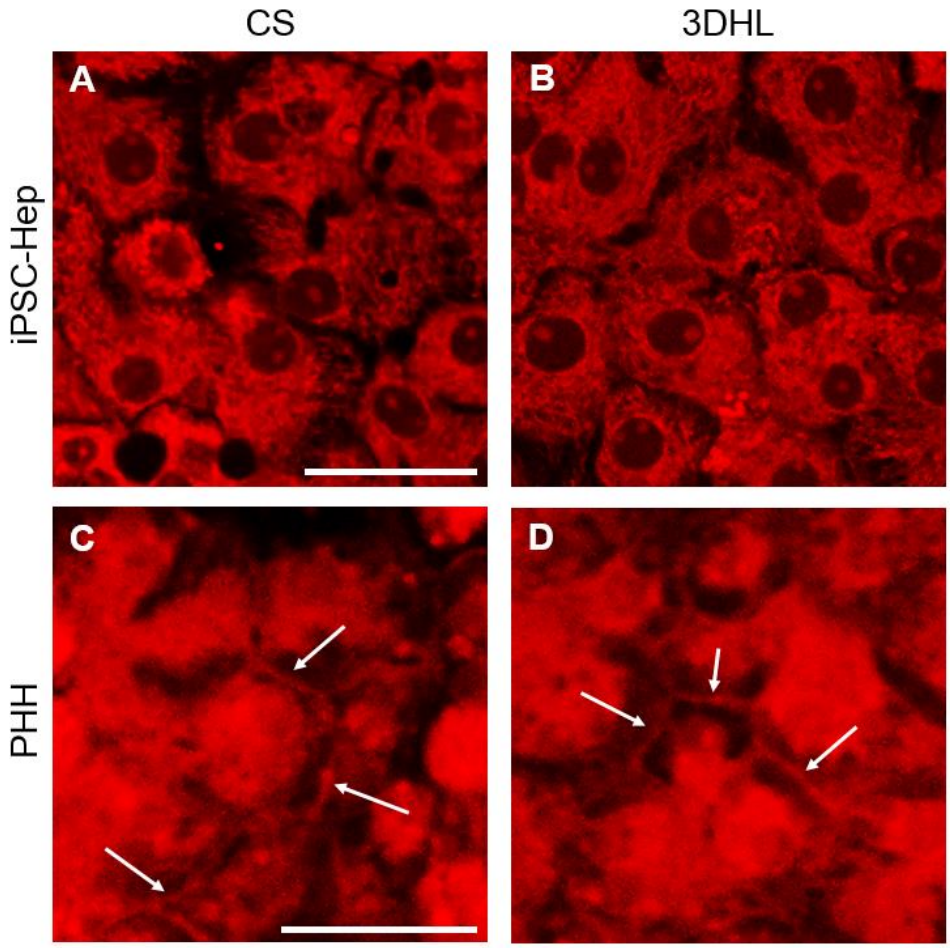

Figure 3.8: Representative images of bile canaliculi formation on day 3 in iPSC-Heps for the (**A)** CS and (**B**) 3DHL models (scale bar = 40 µm). Immunostaining was also completed on day 3 for PHHs in the (**C**) CS and (**D**) 3DHL models (scale bar = 50 µm). White arrows point to examples of bile canaliculi formation.

Synthesis of the serum protein albumin is a primary function of hepatocytes [124]. Hepatocytes rapidly secrete albumin, so presence of intracellular albumin production is a marker of hepatocyte phenotype [124]. Both the iPSC-Heps and the PHHs show albumin production in both culture models. There does not appear to be a difference in albumin production between the CS and 3DHL models for either cell type.

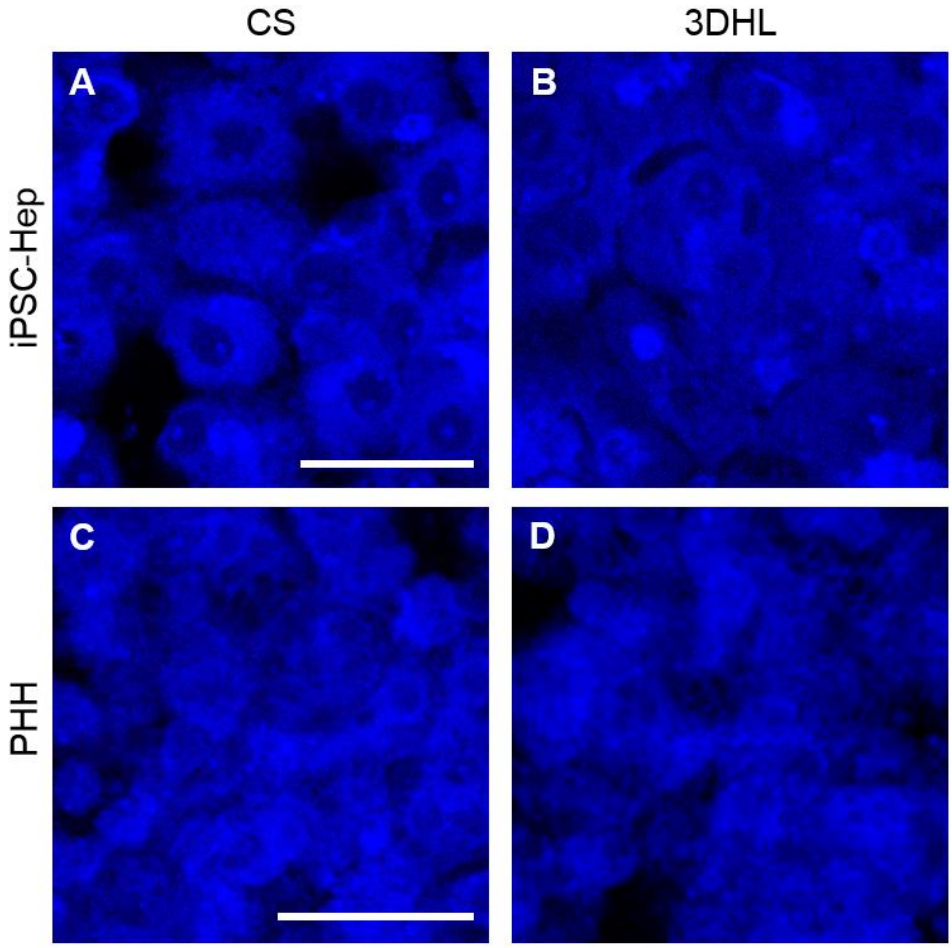

Figure 3.9: Representative images of intracellular albumin production on day 3 in iPSC-Heps in (**A**) CS and (**B**) 3DHL models (scale bar = 40 μm). Immunostaining was also completed for PHHs on day 3 in (**C**) CS and (**D**) 3DHL models (scale bar = 50 μm).

3.3.5 Measuring CYP2E1 Activity in iPSC-Hep and PHH Cultures

CYP2E1 activity was measured by the formation of HFC from the MFC substrate. This particular CYP was analyzed due to its metabolism of different drugs and toxicants. The baseline activity of CYP2E1 for iPSC-Heps in both culture models was 21-27% of the activity value for PHHs (**Figure 3.10**). The PHHs exhibited a statistically significant increase in CYP2E1 activity over iPSC-Heps in the CS model. iPSC-Heps exhibited lower enzymatic function compared to PHHs. For both the iPSC-Heps and PHHs there was no significant increase in CYP2E1 activity when comparing their respective CS and 3DHL cultures.

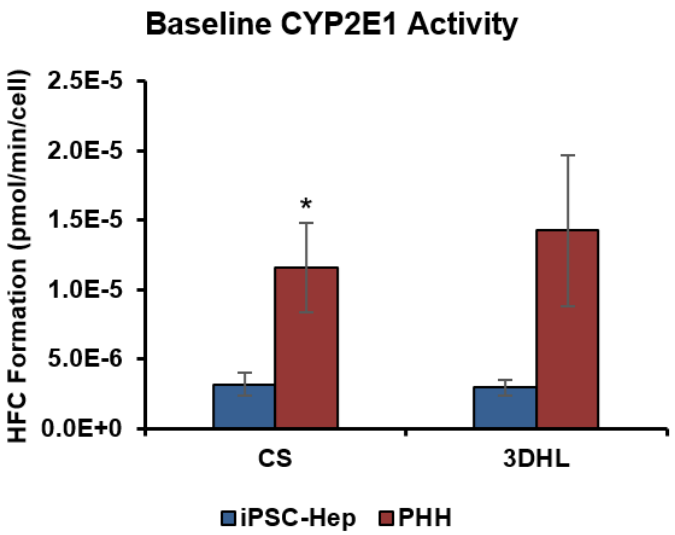

Figure 3.10: CYP2E1 baseline activity for iPSC-Heps and PHHs as both CS and 3DHL models. Activity was measured at day 3 in culture. *$p < 0.05$ relative to the iPSC-Hep values for each respective culture model, $n \geq 3$.

3.3.6 DNA Quantification for CS and 3DHL Models

In iPSC-Heps, CS and 3DHL cultures had 2.88 ± 0.061 and 3.42 ± 0.224 µg/ml of DNA, respectively (**Figure 3.11A**). Although the 3DHL cultures had a significantly higher value of DNA ($p < 0.05$), the percent difference was ~17% indicating the difference may be due to experimental and seeding error. The PHHs also exhibited a statistically significant difference in DNA values between the CS and 3DHL cultures. PHH CS cultures contained 2.92 ± 0.063 µg/ml DNA, while the 3DHL models had 1.57 ± 0.212 µg/ml DNA (**Figure 3.11B**). The PHH 3DHL models exhibited a 46% decrease in DNA compared to the CS models.

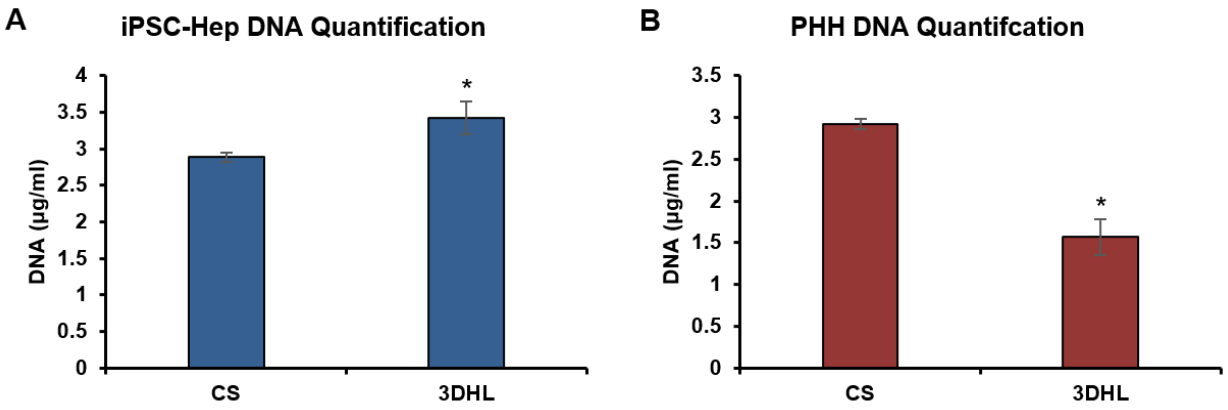

Figure 3.11: DNA quantification for (**A**) iPSC-Heps and (**B**) PHHs in the CS and 3DHL models. Cultures were ended for DNA on Day 3. *$p > 0.05$ relative to the CS models, $n \geq 3$.

3.3.7 Urea Secretion in Response to Toxicants

There is a need to understand how toxicant administration affects hepatic functions. Spent culture media was collected for the day prior to and 24 hours after drug administration to show how urea production was altered by the presence of APAP and EtOH. The urea secretion change is represented as a ratio of the urea production on Day 3 (after administration) to Day 2 (before administration). So a lower urea ratio corresponds to a larger decrease in the urea production at day 3. The iPSC-Hep samples exhibited a statistically significant decrease in urea production with the administration of 2.5 mM and 5 mM APAP (**Figure 3.12A**). No significant change was observed for any of the ethanol administration conditions in the iPSC-Hep CS models. The PHH samples exhibited a statistically significant decrease in urea secretion for both concentrations of APAP (**Figure 3.12B**). This result indicates that both iPSC-Heps and PHHs experienced changes in hepatic function as a result of toxicant administration.

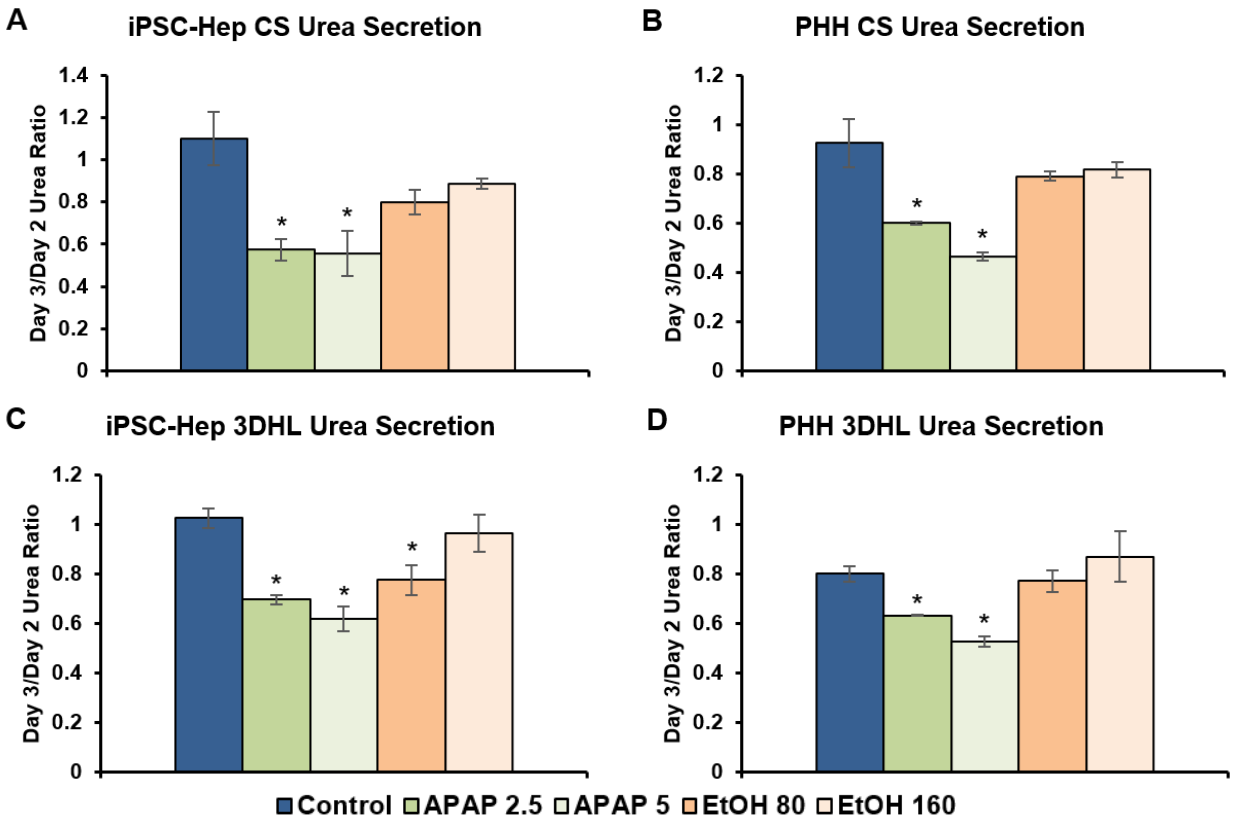

Figure 3.12: Ratio in urea production depicting the amount of urea secretion after drug administration (Day 3) compared to the day before (Day 2). A decrease in the urea ratio corresponds to a decrease in urea production from day 2 to 3. All urea values were normalized to DNA quantity. APAP and EtOH were administered to iPSC-Heps as both (**A**) CS and (**C**) 3DHL cultures. The same administration was completed for PHHs as (**B**) CS and (**D**) 3DHL cultures. All drug concentrations are in mM. *$p < 0.05$ relative to the control, $n = 3$.

The 3DHL iPSC-Hep cultures exhibited statistically significant changes in urea production for all drug administration conditions except for 160 mM EtOH (**Figure 3.12C**). This may indicate the 3DHL culture improved the sensitivity of the iPSC-Heps as there was a significant change in urea production in response to the 80 mM EtOH administration ($p < 0.05$), which was not seen with the CS model. The 3DHL PHH cultures exhibited the same trend as their corresponding CS cultures.

3.3.8 CYP2E1 Activity in CS and 3DHL Cultures Upon Toxicant Administration

To evaluate how drug metabolizing enzyme activity changes with the addition of toxicants, APAP and EtOH were administered to iPSC-Heps and PHHs in CS and 3DHL cultures. CYP2E1 activity was measured 24 hours post-administration. In iPSC-Heps and PHHs as CS cultures the control

CYP2E1 activity was 2.74E-6 ± 7.74E-7 and 9.42E-6 ± 5.53E-7 pmol/min/cell, respectively. iPSC-Heps in the CS model exhibited no statistically significant changes in CYP2E1 activity with toxicant administration (**Figure 3.13 A and C**). When APAP 2.5 mM was administered to the CS cultures the iPSC-Heps and PHHs had activities of 3.01E-6 ± 3.14E-7 and 1.30E-5 ± 7.79E-7 pmol/min/cell, respectively. This was a statistically significant increase in CYP2E1 activity relative to the control samples for the PHHs. A more significant increase in HFC formation in the PHH CS cultures would be expected for the APAP 5 mM concentration but the activity at this condition was 1.13E-5 ± 8.15E-7 pmol/min/cell.

With the addition of the LSECs in the 3DHL cultures the control activity for the iPSC-Heps and PHHs was 2.94E-6 ± 5.84E-7 and 1.43E-5 ± 5.45E-6 pmol/min/cell, respectively. When 80 mM EtOH was administered to the 3DHL iPSC-Hep and PHH cultures the activity values were 1.59E-6 ± 5.30E-8 and 6.38E-6 ± 2.01E-6 pmol/min/cell, respectively. This corresponded to a 42% decrease for the iPSC-Hep cultures and a 55% decrease in the PHHs relative to their controls (**Figure 3.13 C and D**). Similar decreases in activity are shown when APAP 5 mM is administered to the 3DHL models as iPSC-Hep activity for this condition is 2.12E-6 ± 6.87E-7, while the PHH value was 6.82E-6 ± 3.49E-6 pmol/min/cell. This resulted in a 32% decrease in activity for iPSC-Heps, and a 52% decrease for PHHs relative to their controls. This may reflect that the addition of the LSECs with the PHHs are helping the hepatocytes exhibit increased sensitivity to toxicants.

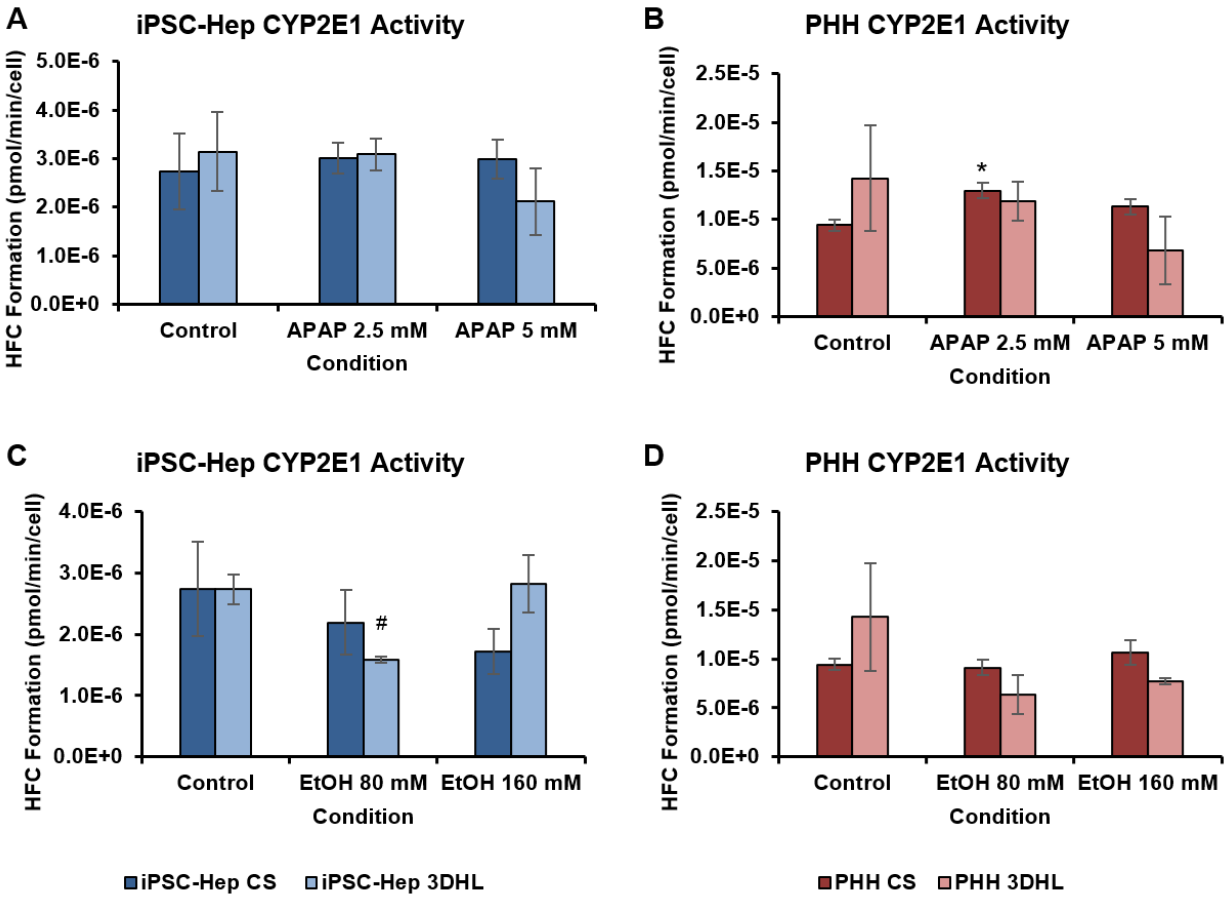

Figure 3.13: Comparison between CS and 3DHL models when toxicants are administered for CYP2E1 activity. Activity was measured 24 hours after drug administration of (**A, B**) APAP and (**C, D**) EtOH. All measurements occurred at day 3. Administration was given for (**A, C**) iPSC-Heps and (**B, D**) PHHs. *p < 0.05 relative to the CS control; #p < 0.05 relative to the 3DHL control, n = 3.

3.3.9 Changes in Mitochondrial Membrane Permeability

The JC-1 assay was used to analyze the integrity of the mitochondrial membrane through the measurement of both healthy and damaged mitochondria. Changes in the cell cultures were assessed through the quantitative ratios of red to green fluorescence. Red dye was a measurement for healthy cells, while the green dye was a marker of lost mitochondrial membrane integrity. So a decrease in the ratio indicates an increase in the damage sustained by the mitochondria. The control ratios of the CS cultures for iPSC-Heps and PHHs was 3.51 ± 1.09 and 1.32 ± 0.043, respectively. Similar ratio values were obtained for the 3DHL cultures of iPSC-Heps and PHHs as the values were 2.78 ± 0.800 and 1.64 ± 0.195, respectively. It is interesting

to note that the ratios of the control samples for iPSC-Heps are ~2 fold higher than the PHH cultures.

When EtOH 160 mM was administered to CS cultures for iPSC-Heps and PHHs, the resulting ratios of mitochondrial membrane integrity were 1.77 ± 0.303 and 1.15 ± 0.137, respectively (**Figure 3.14 B and D**). The iPSC-Hep CS model exhibited a 50% decrease in mitochondrial membrane integrity for this administration condition, while the PHHs only had a 12% decrease. The PHH 3DHL model exhibited a statistically significant decrease in mitochondrial health when 5 mM APAP was administered. In the 3DHL models the iPSC-Hep and PHH ratios with 5 mM APAP was 2.61 ± 0.787 and 1.07 ± 0.048, respectively (**Figure 3.14 A and C**). This corresponded to a 34% decrease in the PHHs and a 6% decrease in the iPSC-Heps.

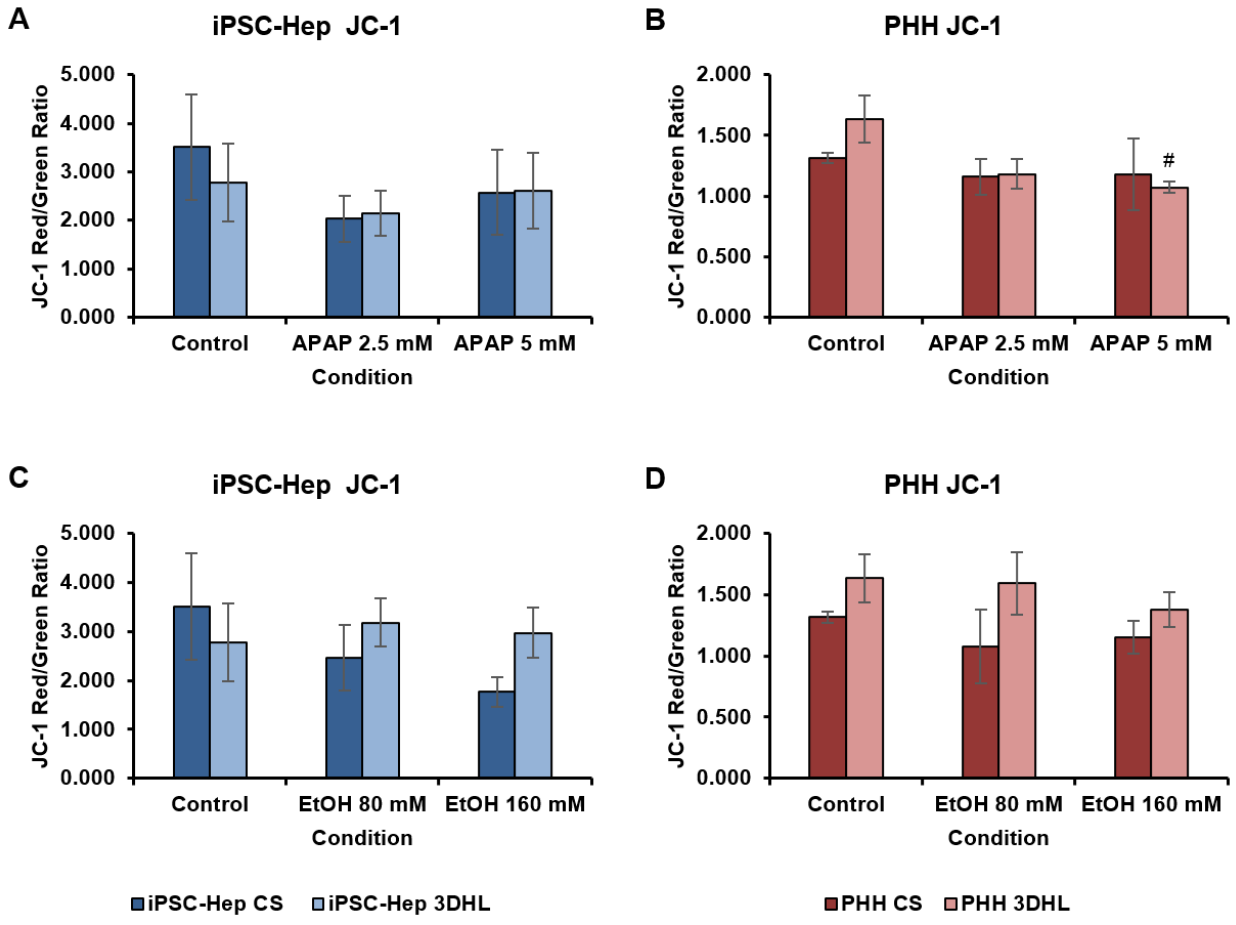

Figure 3.14: Ratios of red to green fluorescence. Red fluorescence is a measurement of healthy cells, while the green fluorescence is a marker for a loss in mitochondrial membrane integrity. A decrease in the ratio corresponds to an increase in the mitochondrial membrane damage. Ratios were calculated for (**A, C**) iPSC-Hep and (**B, D**) PHH cultures for both CS and 3DHL models at Day 3. The two toxicants administered were (**A, B**) APAP and (**C, D**) EtOH. *p < 0.05 relative to the CS controls; #p < 0.05 relative to the 3DHL controls, n = 3.

3.3.10 Evaluation of Changes in Glutathione after Toxicant Administration

GSH was measured 24 hours after toxicant administration. When 160 mM EtOH was administered to the CS cultures, the resulting fold change of GSH in iPSC-Heps was 0.603 ± 0.098 and in PHHs was 2.21 ± 0.687 relative to their controls. This corresponded to a statistically significant 40% decrease in GSH in the iPSC-Hep CS cultures (**Figure 3.15C**). The PHHs showed no significant changes in GSH for any of the drug concentrations in the CS model.

The 3DHL model for iPSC-Heps and PHHs when 80 mM EtOH was administered exhibited a 0.859 ± 0.046 and 0.553 ± 0.100 fold change in GSH, respectively (**Figure 3.15 C and D**). The PHH 3DHL model also exhibited GSH decreases with 2.5 mM and 5 mM APAP administration. The PHH 3DHL fold change in GSH for APAP 2.5 mM and 5 mM was 0.726 ± 0.093 and 0.847 ± 0.140. In the iPSC-Hep 3DHL cultures the fold change in GSH relative to the control was 1.013 ± 0.245 and 1.179 ± 0.419 for 2.5 and 5 mM APAP administration, respectively. The decreases in GSH present in the PHHs in the 3DHL model indicate that the addition of the LSECs are improving the toxic response of the hepatocytes.

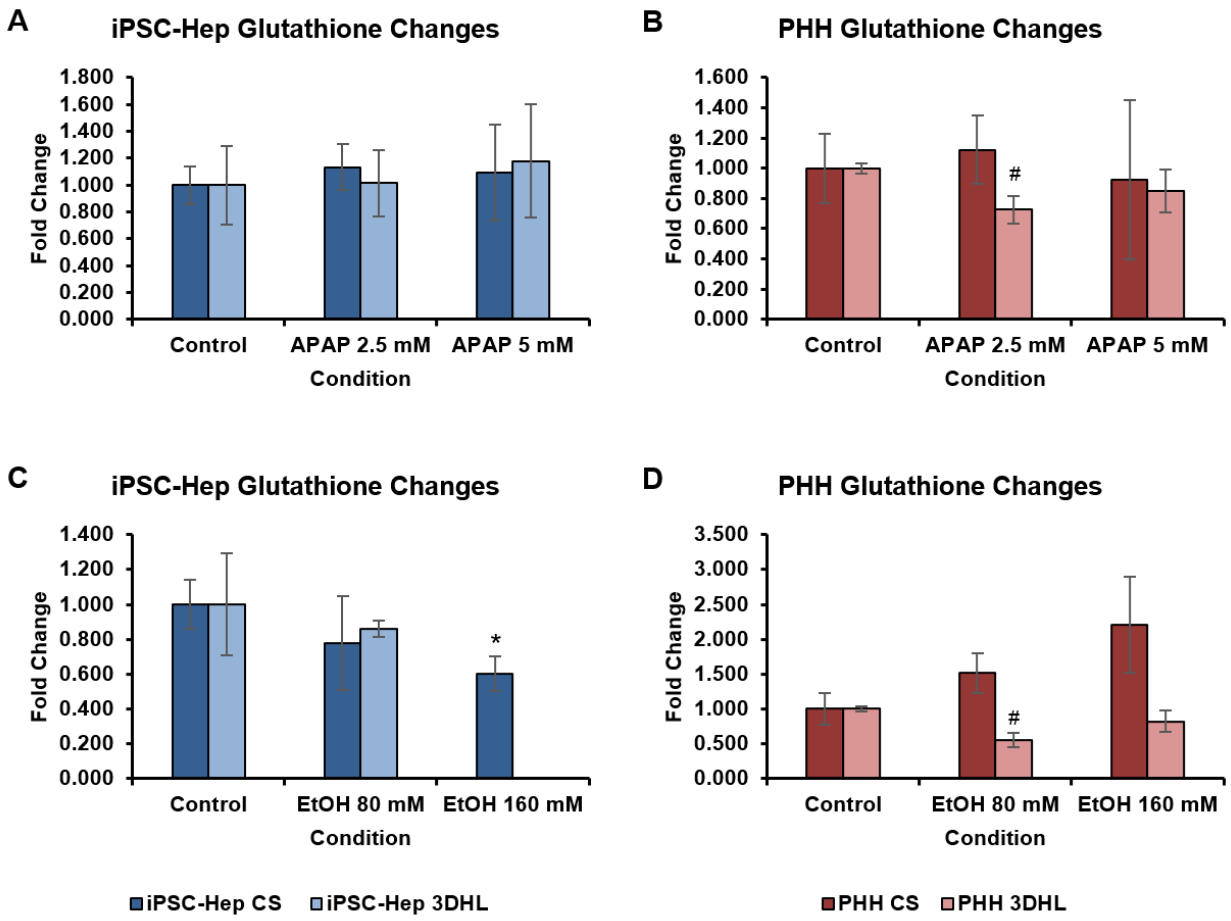

Figure 3.15: Comparison of changes in GSH for (**A, C**) iPSC-Heps and (**B, D**) PHHs relative to the respective controls between CS and 3DHL models. GSH was measured 24 hours after administration of (**A, B**) APAP and (**C, D**) EtOH. *$p < 0.05$ relative to the CS controls; #$p < 0.05$ relative to the 3DHL controls, $n = 3$.

3.4 Discussion

The goal of this study was to understand how introducing an additional hepatic cell type in a 3D *in vitro* culture would impact the functionality of iPSC-Heps. The iPSC-Heps were compared against corresponding PHH models. This study was done in conjunction with PHHs to compare hepatic functions in iPSC-Heps relative to PHHs that are obtained from liver tissue.

iPSC-Hep cell morphology closely resembled the morphology of PHHs, as seen through the representative phase contrast images. The main difference in cellular morphology appeared to

be the cell area, the PHHs had ~40-49% more area than the iPSC-Heps. Prominent protein expression changes were observed for the actin cytoskeleton and bile canaliculi channels. The absence of bile canaliculi formation in the iPSC-Heps indicated these cells were not exhibiting full hepatocyte phenotype. When quantitatively comparing the iPSC-Hep baseline hepatic functions to PHHs, an overall reduction in hepatocyte ability was observed. iPSC-Hep urea production in the CS model was shown to be ~2-2.5 fold lower than PHHs over time in culture. Past publications have reported iPSC-Hep urea secretion to range between ~30% and ~85% of PHH urea secretion [57, 62]. The iPSC-Hep CYP2E1 activity was also only ~21-27% of the PHH activity. Past reports on CYP activity have varied greatly. Regarding CYP2E1 specifically there are conflicting studies in which one report states that iPSC-Hep activity is ~ 4-fold higher than PHH activity, while another reports greatly reduced CYP2E1 expression in iPSC-Heps [60, 80]. The addition of the LSECs in the 3DHL cultures did not improve the baseline iPSC-Hep function, as there was no significant difference in either urea secretion or CYP activity when compared to the CS models. This may be due to the end point analysis only occurring, at most, 2 days after the addition of the top gel containing the LSECs. Phenotypic changes may require additional days in culture until a significant difference is observed. Overall, the iPSC-Heps exhibited various markers of hepatic phenotype such as urea secretion, albumin production, and CYP2E1 activity.

As a main utilization of the iPSC-Hep cells is for hepatotoxicity studies, we administered two well studied hepatotoxicants, APAP and EtOH, to analyze the functional response 24 hours after administration. The impact of the toxicants was measured through CYP2E1 activity, mitochondrial membrane integrity, urea secretion, and glutathione quantity to obtain a broad understanding of the iPSC-Hep response.

Analyzing the changes in urea secretion from day 2 to 3 after toxicant administration occurred, the CS models for both cell types exhibited a significant decrease in urea after APAP

administration. This result demonstrated that the iPSC-Heps were capable of displaying sensitivity to toxins, which was also seen to increase with the addition of the LSECs in the 3DHL model.

When toxins were administered the iPSC-Hep 3DHL cultures appeared to be exhibiting greater changes in CYP2E1 activity relative to the CS cultures. The CYP2E1 activity for iPSC-Hep and PHH 3DHL cultures each decreased 33% and 36%, respectively, at 5 mM APAP. The large decreases in activity observed with these administered conditions may be indicating that cell death was occurring, implying that the presence of the LSECs in the 3DHL culture was increasing the sensitivity of the iPSC-Heps. The large change in activity seen with the 3DHL model was most likely due to the presence of LSECs as they help propagate the toxic response. The PHH CS model did however exhibit a statistically significant increase in activity with 2.5 mM APAP administration. This increase in activity may indicate the presence of ethanol was inducing CYP enzyme expression.

Assessing mitochondrial membrane permeability there appeared to be less change in the membrane integrity in the iPSC-Hep 3DHL model relative to the CS cultures, particularly for ethanol administration. This may show that the LSECs also had a protective effect. In the liver the LSECs line the sinusoids and are the first cells exposed to harmful substances delivered to the liver, making them the initial toxicant recipient. LSECs are reported to exhibit cellular damage prior to parenchymal cell damage, so the LSECs can directly protect the hepatocytes in the early stages of the toxic administration [125, 126].

Changes in glutathione for different administration conditions for the iPSC-Hep CS and 3DHL models were similar to one another, showing decreases when ethanol was administered, but lacked a change with APAP. The PHH 3DHL models exhibited statistically significant decreases

for administration of APAP 2.5 mM and EtOH 80 mM. This trend was not present in the PHH CS culture, implying the 3DHL model was more representative of hepatotoxicity. Depletion of glutathione would be expected during administration of both toxicants as both APAP and EtOH can be metabolized into NAPQI and acetaldehyde, respectively, which are both harmful substances [114]. The production of these reactive metabolites can lead to the depletion of the antioxidant GSH [114, 127]. The absence of GSH depletion in iPSC-Heps could indicate that these cells were not quite mature and lacked full hepatic biochemical pathways.

The iPSC-Heps showed markers of hepatic phenotype in both *in vitro* culture models. Although functionality was seen to be markedly lower compared to PHHs, the iPSC-Heps were capable of exhibiting sensitivity to drug administration. While the 3DHL model did not drastically increase hepatotoxic sensitivity for all analyzed end points, the results show the potential to continue to develop 3D models with the incorporation of other hepatic NPCs.

Chapter 4: Conducting RNA Sequencing of iPSC-Heps and PHHs; Future Directions

4.1 RNA-Seq: Introduction

Many protocols exist to differentiate iPSCs to hepatocytes and although they generally follow the same basic procedure, slight differences may yield a different cell phenotype. In a detailed computational and experimental study conducted by Salomonis *et al*., on 58 iPSCs obtained from 10 different research groups, several concerns were identified [96]. The authors reported several issues with iPSCs such as contamination, formation of teratomas, morphological and karyotypic abnormalities. The concerns raised in this study will require additional experimentation to fully understand how iPSCs may be utilized in tissue engineering and toxicity studies.

A thorough characterization of iPSCs is essential to identify changes that may occur as a result of variations in differentiation protocols, contaminations, gender, DNA methylation and teratoma lineage [96]. While transcriptomic comparisons between ESCs and PHHs have been reported, there is a need to compare iPSC-Heps to adult PHHs. We have prepared samples to conduct RNA-Seq analysis to identify changes at the transcriptomics levels between iPSCs and PHHs. We will use RNA-Seq since this technique can provide detailed information on mRNAs, non-coding RNAs, small RNAs, and post-translational modifications [128]. RNA-Seq is a relatively new technology for transcriptome mapping [128].

The most extensive genetic study completed involving iPSC-Heps was a microarray study comparing iPSC-Heps, PHHs, HepaRG, Huh, and HepG2 cells to directly compare common human hepatic cell types [80]. Gao and Liu reported that in terms of global genome expression iPSC-Heps most closely resembled PHHs, followed by HepaRG [80]. When specifically analyzing

hepatotoxicity related genes HepaRG exhibited the closest relation to PHHs, followed by iPSC-Heps.

In this project our focus is two-fold.

i. Conduct RNA-Seq on iPSC-Heps and PHHs to determine differences.
ii. Conduct RNA-Seq on iPSC-Heps in 3DHL model to determine if the addition of non-parenchymal hepatic cells resulted in a phenotype closer to adult PHHs at different time points.

4.2 RNA-Seq: Materials and Methods

RPMI, B27 supplement, phosphate buffered saline (PBS), Tris-HCl, ethylenediaminetetraacetic acid (EDTA), ethanol, and TrypLE were obtained from Thermo Fisher Scientific (Waltham, MA). Gentamicin, collagenase, β-mercaptoethanol, and sodium dodecyl sulfate (SDS), were purchased from Sigma-Aldrich (St. Louis, MO). Oncostatin M was obtained from R&D systems (Minneapolis, MN). Dexamethasone was purchased from MP Biomedicals (Solon, OH).

4.2.1 Collagen Extraction

Type I collagen was extracted from rat tails, which has been previously described [98-100]. In summary, tendons obtained from rat tails were dissolved in acetic acid. The resulting collagen solution was purified through centrifugation at 13,000 x g and precipitated with 30% (w/v) sodium chloride. Collagen was centrifuged at 8500 x g and the dialyzed in 1 mM hydrochloric acid. The solution was sterilized with chloroform and maintained at a concentration of 2.0–3.0 mg/ml with a pH of 3.1.

4.2.2 iPSC-Hep Cell Cultures

iPSC-Heps were purchased from a commercial source (iCell Hepatocytes 2.0; Cellular Dynamics International (CDI), Madison WI). The iPSC-Heps were differentiated from fibroblasts obtained

from a Caucasian female donor. Cells were received cryopreserved from CDI and were cultured as per the manufacturer's instructions. Upon thawing the cells were plated and maintained until day 4 in manufacturer recommended plating media. Plating media consisted of RPMI supplemented with 20 ng/ml Oncostatin M, 0.1 µM dexamethasone, 5 µg/mL gentamicin, B27 supplement, and iCell Hepatocytes 2.0 medium supplement. On day 5 cells were then maintained in maintenance media containing RPMI, 0.1 µM dexamethasone, 5 µg/mL gentamicin, B27 supplement, and iCell Hepatocytes 2.0 medium supplement.

4.2.3 Primary Human Hepatocyte Cultures

PHHs were obtained from Sekisui XenoTech, LLC (Kansas City, KS). The PHH donor was a 26 year old Caucasian male with a BMI of 26.1 and no known diseases. Cells were received cryopreserved. After thawing and resuspension the cells were originally plated in manufacturer supplied OptiThaw media. The cells were further maintained in manufacturer supplied OptiCulture media.

4.2.4 Culturing Conditions

iPSC-Heps were plated onto type I collagen-coated tissue culture polystyrene (TCPS) well-plates at a manufacturer recommended density of 300,000 cells/cm^2. PHHs were plated onto 1.1 mg/ml type I collagen gels at a concentration of 560,000 cells/well for a 6-well plate. Plating number of PHHs was based upon previously optimized cell densities [114]. Culture medium was changed every 24 hours for both cell cultures. Cells were maintained at 37ºC in a humidified environment at 5% carbon dioxide.

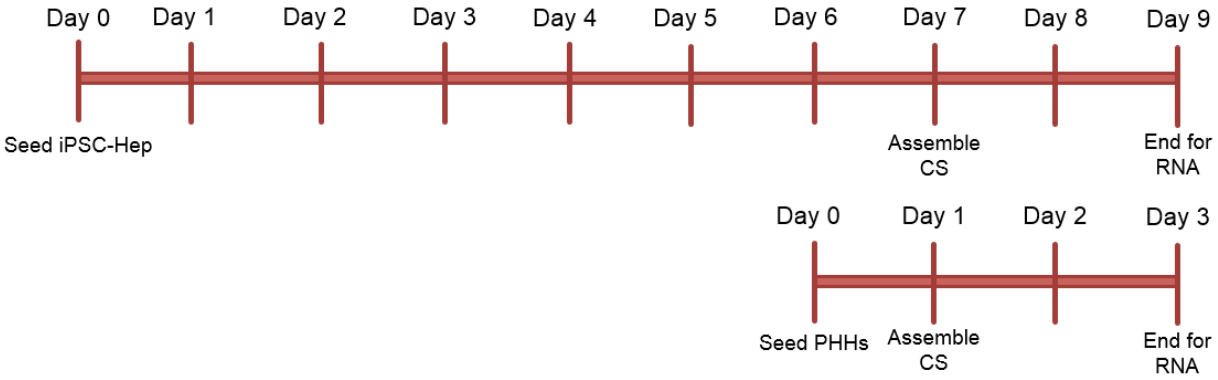

Figure 4.1: Experimental timeline. iPSC-Heps and PHHs were seeded and ended upon different timeline. iPSC-Heps are seeded 6 days prior to the seeding of the PHHs. This is done to align the time points when each cell type can be used for assay.

For use of the iCell Hepatocytes 2.0 the company does not recommend assaying the cells until day 7 (personal communication). The PHHs can be used for assay 24 hours after plating. The PHHs were plated 6 days after the seeding of the iPSC-Heps to align the timeline of the two cell types (**Figure 4.1**). 24 hours after the seeding of the PHHs a 1.1 mg/ml type I collagen solution was added to the cell cultures to form a collagen gel above the monolayer of cells to form a CS culture. Collagen was allowed to form for ~45 minutes at 37ºC and then was hydrated with the respective hepatocyte medium.

4.2.5 RNA Extraction

The RNA extraction process was completed for cells fresh out of the cryopreserved vial (day 0), or on cells that were plated and cultured as previously described. The fresh cell solutions were mixed with RNAprotect Cell Reagent (Qiagen) and stored until extraction. Plated iPSC-Heps were collected on day 9 through the addition of TrypLE and the resulting cell suspension was centrifuged at 800 x g for 2 minutes. The supernatant was aspirated and the remaining pellet was re-suspended in RNAprotect Cell Reagent. A similar process was utilized for the plated PHHs ended on day 3, except cultures were ended through the addition of collagenase.

The RNA extraction was carried out using the RNeasy Plus Micro Kit (Qiagen). The outlined procedure is adopted from the manufacturer's protocol. In summary, the cells suspended in the RNAprotect Cell Reagent were centrifuged for 5 minutes at 5000 x g. The pellet was re-suspended in RLT buffer supplemented with β-mercaptoethanol. The lysate was homogenized using the QIAshredder spin columns. The homogenized lysate was then transferred to the gDNA Eliminator spin column and the resulting flow-through was mixed with 70% ethanol. Solution was centrifuged through the RNeasy MinElute spin column. Buffer RW1, buffer RPE, and 80% ethanol were added sequentially to the spin column. The final RNA collection step was completed by centrifuging 14 µl of RNase-free water through the spin column. Samples were stored at -80ºC.

4.3 RNA-Seq: Results

We have started the work for this portion of the project. All RNA extraction has been completed and a portion of the samples have been sent out for sequencing. Sequencing is being conducted at the Biocomplexity Institute of Virginia Tech. Each sample has been analyzed by the Core Lab facility to determine the RNA integrity number (RIN) (**Table 4.1**). Based upon the RIN results all samples were approved for RNA-Seq, except for one PHH day 3 sample. The approved samples are currently in the process of being sequenced.

Sample ID	Final RIN
iPSC-Hep Day 0 (1)	9.8
iPSC-Hep Day 0 (2)	9.6
iPSC-Hep Day 0 (3)	9.8
iPSC-Hep Day 0 (4)	9.8
iPSC-Hep Day 9 (2)	9.7
iPSC-Hep Day 9 (3)	9.7
iPSC-Hep Day 9 (4)	9.7
PHH Day 0 (1)	7.7
PHH Day 0 (2)	7.7
PHH Day 0 (3)	8.1
PHH Day 0 (4)	8.1
PHH Day 3 (1)	7.6
PHH Day 3 (2)	7.7
PHH Day 3 (3)	7.9
PHH Day 3 (4)	6.4
PHH Day 3 (5)	7.5

Table 4.1: RNA integrity number (RIN) results for iPSC-Hep and PHH samples. iPSC-Heps were collected either upon thaw (Day 0) or as a CS culture (Day 9). PHHs were collected either upon thaw (Day 0) or as a CS culture (Day 3). Green values were approved for sequencing, while the red value failed.

4.4 Kupffer Cells: Future Direction

The 3D culture model described in Chapter 3 involved the addition of another hepatic cell type, LSECs, to develop a 3D *in vitro* model that was more representative of the liver tissue architecture. While the LSECs are an important and prominent cell type in the liver, they alone cannot accurately represent the inter-cellular communication present during hepatotoxicity. Kupffer cells are the resident macrophages of the liver [40]. These cells can become activated when in the presence of a toxicant and as a result will release cytokines and reactive oxygen species (ROS) [129]. The cytokines can be both pro/anti-inflammatory mediators and can greatly help aid in the progression of hepatocellular injury due to drug administration [98, 129]. Past studies involving the addition of both LSECs and Kupffer cells saw better sensitivity towards hepatotoxicants and a hepatic response that was more indicative of *in vivo* results [98, 114]. To achieve better iPSC-Hep response to toxicants it is important that the Kupffer cells are integrated into the model.

Upcoming studies will incorporate human Kupffer cells into the 3DHL model to develop 3DHLK cultures and analyze the hepatotoxic response in comparison to PHHs.

References

1. Murry, C.E. and G. Keller, *Differentiation of embryonic stem cells to clinically relevant populations: lessons from embryonic development.* Cell, 2008. **132**(4): p. 661-80.
2. Romito, A. and G. Cobellis, *Pluripotent Stem Cells: Current Understanding and Future Directions.* Stem Cells Int, 2016. **2016**: p. 9451492.
3. Odorico, J.S., D.S. Kaufman, and J.A. Thomson, *Multilineage differentiation from human embryonic stem cell lines.* Stem Cells, 2001. **19**(3): p. 193-204.
4. Wobus, A.M. and K.R. Boheler, *Embryonic stem cells: prospects for developmental biology and cell therapy.* Physiol Rev, 2005. **85**(2): p. 635-78.
5. Gan, Q., et al., *Concise review: epigenetic mechanisms contribute to pluripotency and cell lineage determination of embryonic stem cells.* Stem Cells, 2007. **25**(1): p. 2-9.
6. Thomson, J.A., et al., *Embryonic stem cell lines derived from human blastocysts.* Science, 1998. **282**(5391): p. 1145-7.
7. Mummery, C., et al., *Stem cells: scientific facts and fiction*. 2014: Academic Press.
8. Jaenisch, R. and R. Young, *Stem cells, the molecular circuitry of pluripotency and nuclear reprogramming.* Cell, 2008. **132**(4): p. 567-82.
9. Amabile, G. and A. Meissner, *Induced pluripotent stem cells: current progress and potential for regenerative medicine.* Trends Mol Med, 2009. **15**(2): p. 59-68.
10. Takahashi, K., et al., *Induction of pluripotent stem cells from adult human fibroblasts by defined factors.* Cell, 2007. **131**(5): p. 861-72.
11. Takahashi, K. and S. Yamanaka, *Induction of pluripotent stem cells from mouse embryonic and adult fibroblast cultures by defined factors.* Cell, 2006. **126**(4): p. 663-76.
12. Shi, Y., et al., *A combined chemical and genetic approach for the generation of induced pluripotent stem cells.* Cell Stem Cell, 2008. **2**(6): p. 525-8.
13. Yu, J., et al., *Induced pluripotent stem cell lines derived from human somatic cells.* Science, 2007. **318**(5858): p. 1917-20.
14. Nakagawa, M., et al., *Generation of induced pluripotent stem cells without Myc from mouse and human fibroblasts.* Nat Biotechnol, 2008. **26**(1): p. 101-6.
15. Maherali, N., et al., *Directly reprogrammed fibroblasts show global epigenetic remodeling and widespread tissue contribution.* Cell Stem Cell, 2007. **1**(1): p. 55-70.
16. Meissner, A., M. Wernig, and R. Jaenisch, *Direct reprogramming of genetically unmodified fibroblasts into pluripotent stem cells.* Nat Biotechnol, 2007. **25**(10): p. 1177-81.
17. Okita, K., T. Ichisaka, and S. Yamanaka, *Generation of germline-competent induced pluripotent stem cells.* Nature, 2007. **448**(7151): p. 313-7.
18. Wernig, M., et al., *In vitro reprogramming of fibroblasts into a pluripotent ES-cell-like state.* Nature, 2007. **448**(7151): p. 318-24.
19. Sommer, C.A., et al., *Induced pluripotent stem cell generation using a single lentiviral stem cell cassette.* Stem Cells, 2009. **27**(3): p. 543-9.
20. Stadtfeld, M. and K. Hochedlinger, *Induced pluripotency: history, mechanisms, and applications.* Genes Dev, 2010. **24**(20): p. 2239-63.
21. Chin, M.H., et al., *Induced pluripotent stem cells and embryonic stem cells are distinguished by gene expression signatures.* Cell Stem Cell, 2009. **5**(1): p. 111-23.
22. Maherali, N. and K. Hochedlinger, *Guidelines and techniques for the generation of induced pluripotent stem cells.* Cell Stem Cell, 2008. **3**(6): p. 595-605.
23. Stadtfeld, M., et al., *Induced pluripotent stem cells generated without viral integration.* Science, 2008. **322**(5903): p. 945-9.
24. Kim, D., et al., *Generation of human induced pluripotent stem cells by direct delivery of reprogramming proteins.* Cell Stem Cell, 2009. **4**(6): p. 472-6.

25. Zhou, H., et al., *Generation of induced pluripotent stem cells using recombinant proteins.* Cell Stem Cell, 2009. **4**(5): p. 381-4.
26. Huangfu, D., et al., *Induction of pluripotent stem cells by defined factors is greatly improved by small-molecule compounds.* Nat Biotechnol, 2008. **26**(7): p. 795-7.
27. Shi, Y., et al., *Induction of pluripotent stem cells from mouse embryonic fibroblasts by Oct4 and Klf4 with small-molecule compounds.* Cell Stem Cell, 2008. **3**(5): p. 568-74.
28. Feng, B., et al., *Molecules that promote or enhance reprogramming of somatic cells to induced pluripotent stem cells.* Cell Stem Cell, 2009. **4**(4): p. 301-12.
29. Rao, L., et al., *Engineering human pluripotent stem cells into a functional skeletal muscle tissue.* Nat Commun, 2018. **9**(1): p. 126.
30. Abud, E.M., et al., *iPSC-Derived Human Microglia-like Cells to Study Neurological Diseases.* Neuron, 2017. **94**(2): p. 278-293 e9.
31. Zhang, J., et al., *Functional cardiomyocytes derived from human induced pluripotent stem cells.* Circ Res, 2009. **104**(4): p. e30-41.
32. Lian, X., et al., *Robust cardiomyocyte differentiation from human pluripotent stem cells via temporal modulation of canonical Wnt signaling.* Proc Natl Acad Sci U S A, 2012. **109**(27): p. E1848-57.
33. Burridge, P.W., et al., *A universal system for highly efficient cardiac differentiation of human induced pluripotent stem cells that eliminates interline variability.* PLoS One, 2011. **6**(4): p. e18293.
34. Karumbayaram, S., et al., *Directed differentiation of human-induced pluripotent stem cells generates active motor neurons.* Stem Cells, 2009. **27**(4): p. 806-11.
35. Kim, D.S., et al., *Robust enhancement of neural differentiation from human ES and iPS cells regardless of their innate difference in differentiation propensity.* Stem Cell Rev, 2010. **6**(2): p. 270-81.
36. Chambers, S.M., et al., *Highly efficient neural conversion of human ES and iPS cells by dual inhibition of SMAD signaling.* Nat Biotechnol, 2009. **27**(3): p. 275-80.
37. Grigoriadis, A.E., et al., *Directed differentiation of hematopoietic precursors and functional osteoclasts from human ES and iPS cells.* Blood, 2010. **115**(14): p. 2769-76.
38. de Peppo, G.M., et al., *Engineering bone tissue substitutes from human induced pluripotent stem cells.* Proc Natl Acad Sci U S A, 2013. **110**(21): p. 8680-5.
39. Liu, J., et al., *Reprogramming of mesenchymal stem cells derived from iPSCs seeded on biofunctionalized calcium phosphate scaffold for bone engineering.* Biomaterials, 2013. **34**(32): p. 7862-72.
40. Arias, I.M., et al., *The Liver: Biology and Pathobiology, fourth ed.* 2001, Philadelphia, PA: Lippincott Williams & Wilkins.
41. Rodés, J., et al., *Textbook of Hepatology: From Basic Science to Clinical Practice. 3rd ed.* 2008, Wiley-Blackwell: Malden, MA.
42. Godoy, P., et al., *Recent advances in 2D and 3D in vitro systems using primary hepatocytes, alternative hepatocyte sources and non-parenchymal liver cells and their use in investigating mechanisms of hepatotoxicity, cell signaling and ADME.* Arch Toxicol, 2013. **87**(8): p. 1315-530.
43. Gomez-Lechon, M.J. and L. Tolosa, *Human hepatocytes derived from pluripotent stem cells: a promising cell model for drug hepatotoxicity screening.* Arch Toxicol, 2016. **90**(9): p. 2049-2061.
44. Schwartz, R.E., et al., *Pluripotent stem cell-derived hepatocyte-like cells.* Biotechnol Adv, 2014. **32**(2): p. 504-13.
45. Si-Tayeb, K., et al., *Highly efficient generation of human hepatocyte-like cells from induced pluripotent stem cells.* Hepatology, 2010. **51**(1): p. 297-305.
46. Song, Z., et al., *Efficient generation of hepatocyte-like cells from human induced pluripotent stem cells.* Cell Res, 2009. **19**(11): p. 1233-42.

47. Sullivan, G.J., et al., *Generation of functional human hepatic endoderm from human induced pluripotent stem cells.* Hepatology, 2010. **51**(1): p. 329-35.
48. Chen, Y.F., et al., *Rapid generation of mature hepatocyte-like cells from human induced pluripotent stem cells by an efficient three-step protocol.* Hepatology, 2012. **55**(4): p. 1193-203.
49. Hannan, N.R., et al., *Production of hepatocyte-like cells from human pluripotent stem cells.* Nat Protoc, 2013. **8**(2): p. 430-7.
50. Palakkan, A.A., J. Nanda, and J.A. Ross, *Pluripotent stem cells to hepatocytes, the journey so far.* Biomed Rep, 2017. **6**(4): p. 367-373.
51. Takayama, K., et al., *Efficient generation of functional hepatocytes from human embryonic stem cells and induced pluripotent stem cells by HNF4alpha transduction.* Mol Ther, 2012. **20**(1): p. 127-37.
52. Gieseck, R.L., 3rd, et al., *Maturation of induced pluripotent stem cell derived hepatocytes by 3D-culture.* PLoS One, 2014. **9**(1): p. e86372.
53. Takayama, K., et al., *3D spheroid culture of hESC/hiPSC-derived hepatocyte-like cells for drug toxicity testing.* Biomaterials, 2013. **34**(7): p. 1781-9.
54. Pettinato, G., et al., *Scalable Differentiation of Human iPSCs in a Multicellular Spheroid-based 3D Culture into Hepatocyte-like Cells through Direct Wnt/beta-catenin Pathway Inhibition.* Sci Rep, 2016. **6**: p. 32888.
55. Koui, Y., et al., *An In Vitro Human Liver Model by iPSC-Derived Parenchymal and Non-parenchymal Cells.* Stem Cell Reports, 2017. **9**(2): p. 490-498.
56. Nagamoto, Y., et al., *The promotion of hepatic maturation of human pluripotent stem cells in 3D co-culture using type I collagen and Swiss 3T3 cell sheets.* Biomaterials, 2012. **33**(18): p. 4526-34.
57. Berger, D.R., et al., *Enhancing the functional maturity of induced pluripotent stem cell-derived human hepatocytes by controlled presentation of cell-cell interactions in vitro.* Hepatology, 2015. **61**(4): p. 1370-81.
58. Wang, B., et al., *Functional Maturation of Induced Pluripotent Stem Cell Hepatocytes in Extracellular Matrix-A Comparative Analysis of Bioartificial Liver Microenvironments.* Stem Cells Transl Med, 2016. **5**(9): p. 1257-67.
59. Du, C., et al., *Induced pluripotent stem cell-derived hepatocytes and endothelial cells in multi-component hydrogel fibers for liver tissue engineering.* Biomaterials, 2014. **35**(23): p. 6006-14.
60. Lu, J., et al., *Morphological and Functional Characterization and Assessment of iPSC-Derived Hepatocytes for In Vitro Toxicity Testing.* Toxicol Sci, 2015. **147**(1): p. 39-54.
61. Medine, C.N., et al., *Developing high-fidelity hepatotoxicity models from pluripotent stem cells.* Stem Cells Transl Med, 2013. **2**(7): p. 505-9.
62. Kang, S.J., et al., *Chemically induced hepatotoxicity in human stem cell-induced hepatocytes compared with primary hepatocytes and HepG2.* Cell Biol Toxicol, 2016. **32**(5): p. 403-17.
63. Coll, M., et al., *Generation of Hepatic Stellate Cells from Human Pluripotent Stem Cells Enables In Vitro Modeling of Liver Fibrosis.* Cell Stem Cell, 2018. **23**(1): p. 101-113 e7.
64. Tasnim, F., et al., *Generation of mature kupffer cells from human induced pluripotent stem cells.* Biomaterials, 2019. **192**: p. 377-391.
65. Kaplowitz, N. and L.D. DeLeve, *Drug-Induced Liver Disease, third ed.* 2013, Waltham, MA: Academic Press.
66. Orbach, S.M., et al., *In Vitro Intestinal and Liver Models for Toxicity Testing.* ACS Biomaterials Science & Engineering, 2017. **3**(9): p. 1898-1910.
67. Soldatow, V.Y., et al., *In vitro models for liver toxicity testing.* Toxicol Res (Camb), 2013. **2**(1): p. 23-39.

68. Astashkina, A., B. Mann, and D.W. Grainger, *A critical evaluation of in vitro cell culture models for high-throughput drug screening and toxicity.* Pharmacol Ther, 2012. **134**(1): p. 82-106.
69. LeCluyse, E.L., et al., *Organotypic liver culture models: meeting current challenges in toxicity testing.* Crit Rev Toxicol, 2012. **42**(6): p. 501-48.
70. Mann, D.A., *Human induced pluripotent stem cell-derived hepatocytes for toxicology testing.* Expert Opin Drug Metab Toxicol, 2015. **11**(1): p. 1-5.
71. Gomez-Lechon, M.J., et al., *Competency of different cell models to predict human hepatotoxic drugs.* Expert Opin Drug Metab Toxicol, 2014. **10**(11): p. 1553-68.
72. Hewitt, N.J., et al., *Primary hepatocytes: current understanding of the regulation of metabolic enzymes and transporter proteins, and pharmaceutical practice for the use of hepatocytes in metabolism, enzyme induction, transporter, clearance, and hepatotoxicity studies.* Drug Metab Rev, 2007. **39**(1): p. 159-234.
73. Vorrink, S.U., et al., *Endogenous and xenobiotic metabolic stability of primary human hepatocytes in long-term 3D spheroid cultures revealed by a combination of targeted and untargeted metabolomics.* FASEB J, 2017. **31**(6): p. 2696-2708.
74. Yoon No, D., et al., *3D liver models on a microplatform: well-defined culture, engineering of liver tissue and liver-on-a-chip.* Lab Chip, 2015. **15**(19): p. 3822-37.
75. Lauschke, V.M., et al., *Novel 3D Culture Systems for Studies of Human Liver Function and Assessments of the Hepatotoxicity of Drugs and Drug Candidates.* Chem Res Toxicol, 2016. **29**(12): p. 1936-1955.
76. Underhill, G.H. and S.R. Khetani, *Bioengineered Liver Models for Drug Testing and Cell Differentiation Studies.* Cell Mol Gastroenterol Hepatol, 2018. **5**(3): p. 426-439 e1.
77. Goldring, C., et al., *Stem cell-derived models to improve mechanistic understanding and prediction of human drug-induced liver injury.* Hepatology, 2017. **65**(2): p. 710-721.
78. Sjogren, A.K., et al., *Critical differences in toxicity mechanisms in induced pluripotent stem cell-derived hepatocytes, hepatic cell lines and primary hepatocytes.* Arch Toxicol, 2014. **88**(7): p. 1427-37.
79. Ware, B.R., D.R. Berger, and S.R. Khetani, *Prediction of Drug-Induced Liver Injury in Micropatterned Co-cultures Containing iPSC-Derived Human Hepatocytes.* Toxicol Sci, 2015. **145**(2): p. 252-62.
80. Gao, X. and Y. Liu, *A transcriptomic study suggesting human iPSC-derived hepatocytes potentially offer a better in vitro model of hepatotoxicity than most hepatoma cell lines.* Cell Biol Toxicol, 2017. **33**(4): p. 407-421.
81. Ulvestad, M., et al., *Drug metabolizing enzyme and transporter protein profiles of hepatocytes derived from human embryonic and induced pluripotent stem cells.* Biochem Pharmacol, 2013. **86**(5): p. 691-702.
82. Smutny, T., et al., *A feasibility study of the toxic responses of human induced pluripotent stem cell-derived hepatocytes to phytochemicals.* Toxicol In Vitro, 2018. **52**: p. 94-105.
83. Chalasani, N., et al., *Causes, clinical features, and outcomes from a prospective study of drug-induced liver injury in the United States.* Gastroenterology, 2008. **135**(6): p. 1924-34, 1934 e1-4.
84. Grimm, F.A., et al., *High-Content Assay Multiplexing for Toxicity Screening in Induced Pluripotent Stem Cell-Derived Cardiomyocytes and Hepatocytes.* Assay Drug Dev Technol, 2015. **13**(9): p. 529-46.
85. Sirenko, O., et al., *High-content assays for hepatotoxicity using induced pluripotent stem cell-derived cells.* Assay Drug Dev Technol, 2014. **12**(1): p. 43-54.
86. Sirenko, O., et al., *Phenotypic Characterization of Toxic Compound Effects on Liver Spheroids Derived from iPSC Using Confocal Imaging and Three-Dimensional Image Analysis.* Assay Drug Dev Technol, 2016. **14**(7): p. 381-94.

87. Holmgren, G., et al., *Long-term chronic toxicity testing using human pluripotent stem cell-derived hepatocytes.* Drug Metab Dispos, 2014. **42**(9): p. 1401-6.
88. Bell, C.C., et al., *Transcriptional, Functional, and Mechanistic Comparisons of Stem Cell-Derived Hepatocytes, HepaRG Cells, and Three-Dimensional Human Hepatocyte Spheroids as Predictive In Vitro Systems for Drug-Induced Liver Injury.* Drug Metab Dispos, 2017. **45**(4): p. 419-429.
89. Takayama, K., et al., *Prediction of interindividual differences in hepatic functions and drug sensitivity by using human iPS-derived hepatocytes.* Proc Natl Acad Sci U S A, 2014. **111**(47): p. 16772-7.
90. Ingelman-Sundberg, M., *Genetic susceptibility to adverse effects of drugs and environmental toxicants. The role of the CYP family of enzymes.* Mutat Res, 2001. **482**(1-2): p. 11-9.
91. Zhou, S.F., *Polymorphism of human cytochrome P450 2D6 and its clinical significance: Part I.* Clin Pharmacokinet, 2009. **48**(11): p. 689-723.
92. Park, I.H., et al., *Disease-specific induced pluripotent stem cells.* Cell, 2008. **134**(5): p. 877-86.
93. Rashid, S.T., et al., *Modeling inherited metabolic disorders of the liver using human induced pluripotent stem cells.* J Clin Invest, 2010. **120**(9): p. 3127-36.
94. Li, S., et al., *Valproic acid-induced hepatotoxicity in Alpers syndrome is associated with mitochondrial permeability transition pore opening-dependent apoptotic sensitivity in an induced pluripotent stem cell model.* Hepatology, 2015. **61**(5): p. 1730-9.
95. Cayo, M.A., et al., *A Drug Screen using Human iPSC-Derived Hepatocyte-like Cells Reveals Cardiac Glycosides as a Potential Treatment for Hypercholesterolemia.* Cell Stem Cell, 2017. **20**(4): p. 478-489 e5.
96. Salomonis, N., et al., *Integrated Genomic Analysis of Diverse Induced Pluripotent Stem Cells from the Progenitor Cell Biology Consortium.* Stem Cell Reports, 2016. **7**(1): p. 110-25.
97. Kia, R., et al., *Stem cell-derived hepatocytes as a predictive model for drug-induced liver injury: are we there yet?* 2013. **75**(4): p. 885-896.
98. Orbach, S.M., et al., *Investigating acetaminophen hepatotoxicity in multi-cellular organotypic liver models.* Toxicol In Vitro, 2017. **42**: p. 10-20.
99. Cassin, M.E., et al., *The design of antimicrobial LL37-modified collagen-hyaluronic acid detachable multilayers.* Acta Biomater, 2016. **40**: p. 119-129.
100. Ford, A.J., G. Jain, and P. Rajagopalan, *Designing a fibrotic microenvironment to investigate changes in human liver sinusoidal endothelial cell function.* Acta Biomater, 2015. **24**: p. 220-7.
101. Chiang, J., *Liver Physiology: Metabolism and Detoxification.* Pathobiology of Human Disease: A Dynamic Encyclopedia of Disease Mechanisms, 2014: p. 1770-1782.
102. Rui, L., *Energy metabolism in the liver.* Compr Physiol, 2014. **4**(1): p. 177-97.
103. Gissen, P. and I.M. Arias, *Structural and functional hepatocyte polarity and liver disease.* J Hepatol, 2015. **63**(4): p. 1023-37.
104. Wagener, G., *Liver anesthesiology and critical care medicine*. 2012: Springer Science & Business Media.
105. Poisson, J., et al., *Liver sinusoidal endothelial cells: Physiology and role in liver diseases.* J Hepatol, 2017. **66**(1): p. 212-227.
106. Dixon, L.J., et al., *Kupffer cells in the liver.* Compr Physiol, 2013. **3**(2): p. 785-97.
107. Yin, C., et al., *Hepatic stellate cells in liver development, regeneration, and cancer.* J Clin Invest, 2013. **123**(5): p. 1902-10.
108. Baze, A., et al., *Three-Dimensional Spheroid Primary Human Hepatocytes in Monoculture and Coculture with Nonparenchymal Cells.* Tissue Eng Part C Methods, 2018. **24**(9): p. 534-545.

109. Nguyen, D.G., et al., *Bioprinted 3D Primary Liver Tissues Allow Assessment of Organ-Level Response to Clinical Drug Induced Toxicity In Vitro.* PLoS One, 2016. **11**(7): p. e0158674.
110. Prodanov, L., et al., *Long-term maintenance of a microfluidic 3D human liver sinusoid.* Biotechnol Bioeng, 2016. **113**(1): p. 241-6.
111. Messner, S., et al., *Multi-cell type human liver microtissues for hepatotoxicity testing.* Arch Toxicol, 2013. **87**(1): p. 209-13.
112. Proctor, W.R., et al., *Utility of spherical human liver microtissues for prediction of clinical drug-induced liver injury.* Arch Toxicol, 2017. **91**(8): p. 2849-2863.
113. Bell, C.C., et al., *Characterization of primary human hepatocyte spheroids as a model system for drug-induced liver injury, liver function and disease.* Sci Rep, 2016. **6**: p. 25187.
114. Orbach, S.M., M.F. Ehrich, and P. Rajagopalan, *High-throughput toxicity testing of chemicals and mixtures in organotypic multi-cellular cultures of primary human hepatic cells.* Toxicol In Vitro, 2018. **51**: p. 83-94.
115. Kola, I. and J. Landis, *Can the pharmaceutical industry reduce attrition rates?* Nat Rev Drug Discov, 2004. **3**(8): p. 711-5.
116. Corsini, A., et al., *Current challenges and controversies in drug-induced liver injury.* Drug Saf, 2012. **35**(12): p. 1099-117.
117. Kaitin, K.I., *Deconstructing the drug development process: the new face of innovation.* Clin Pharmacol Ther, 2010. **87**(3): p. 356-61.
118. Larkin, A.L., et al., *Designing a multicellular organotypic 3D liver model with a detachable, nanoscale polymeric Space of Disse.* Tissue Eng Part C Methods, 2013. **19**(11): p. 875-84.
119. Klaassen, C.D., *Casarett & Doull's Toxicology: The Basic Science of Poisons, Eighth Edition*. 2013, New York, NY: McGraw-Hill.
120. Donato, M.T., et al., *Fluorescence-based assays for screening nine cytochrome P450 (P450) activities in intact cells expressing individual human P450 enzymes.* Drug Metab Dispos, 2004. **32**(7): p. 699-706.
121. Mingoia, R.T., et al., *Primary culture of rat hepatocytes in 96-well plates: effects of extracellular matrix configuration on cytochrome P450 enzyme activity and inducibility, and its application in in vitro cytotoxicity screening.* Toxicol In Vitro, 2007. **21**(1): p. 165-73.
122. Kim, Y., et al., *The design of in vitro liver sinusoid mimics using chitosan-hyaluronic acid polyelectrolyte multilayers.* Tissue Eng Part A, 2010. **16**(9): p. 2731-41.
123. Detzel, C.J., Y. Kim, and P. Rajagopalan, *Engineered three-dimensional liver mimics recapitulate critical rat-specific bile acid pathways.* Tissue Eng Part A, 2011. **17**(5-6): p. 677-89.
124. Rothschild, M.A., M. Oratz, and S.S. Schreiber, *Serum albumin.* Hepatology, 1988. **8**(2): p. 385-401.
125. Sorensen, K.K., et al., *Liver Sinusoidal Endothelial Cells.* Compr Physiol, 2015. **5**(4): p. 1751-74.
126. Ito, Y., et al., *Early hepatic microvascular injury in response to acetaminophen toxicity.* Microcirculation, 2003. **10**(5): p. 391-400.
127. Jaeschke, H., et al., *Mechanisms of hepatotoxicity.* Toxicol Sci, 2002. **65**(2): p. 166-76.
128. Wang, Z., M. Gerstein, and M. Snyder, *RNA-Seq: a revolutionary tool for transcriptomics.* Nat Rev Genet, 2009. **10**(1): p. 57-63.
129. Kolios, G., V. Valatas, and E. Kouroumalis, *Role of Kupffer cells in the pathogenesis of liver disease.* World J Gastroenterol, 2006. **12**(46): p. 7413-20.